AD-A163 563 A RECURSIVE BOUNDARY ELEMENT WITH INITIAL ERROR INVESTIGATION(U) NAVAL CIVIL ENGINEERING LAB PORT HUENEME CA J V COX ET AL DEC 85 NCEL-TN-1730 1/1

UNCLASSIFIED F/G 12/1 NL

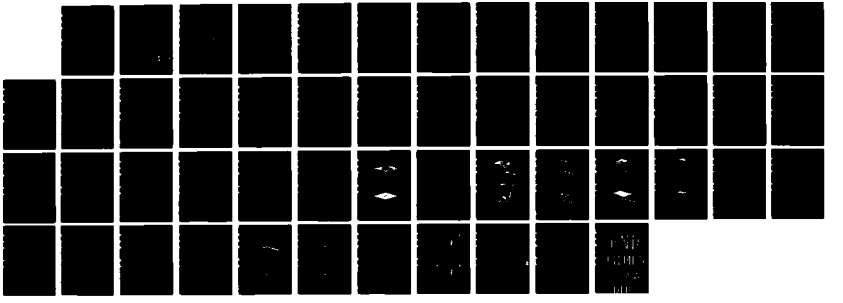

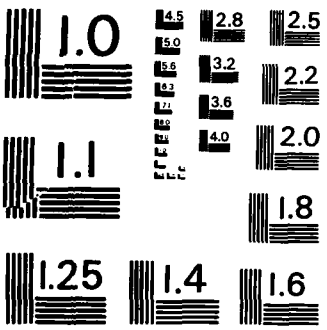

MICROCOPY RESOLUTION TEST CHART

NATIONAL BUREAU OF STANDARDS - 1963 - A

(12)

N-1730
December 1985

NCEL
Technical Note

By J.V. Cox and T.A. Shugar

Sponsored By Naval Facilities
Engineering Command

A RECURSIVE BOUNDARY ELEMENT WITH INITIAL ERROR INVESTIGATION

ABSTRACT **A recursive numerical integration technique is developed for the boundary element method. The initial implementation is within an indirect formulation for two-dimensional elastostatics. A numerical study investigates the error field near a single boundary element in the infinite plane using different orders of numerical integration. The difficulty of integrating the singular kernal functions with discrete integration points is eliminated with a recursive algorithm that adaptively subdivides elements that are in close proximity to the internal response point. The recursive technique allows calculation of internal responses arbitrarily close to the boundary with no loss of accuracy. This frees the analyst to design the boundary subdivision based on boundary geometry and anticipated boundary response gradients without regard for the numerical integration accuracy of responses near the boundary. The gradient of the artificial tractions must ordinarily be considered when modeling problems with the indirect formulation.**

NAVAL CIVIL ENGINEERING LABORATORY PORT HUENEME CALIFORNIA 93043

METRIC CONVERSION FACTORS

Approximate Conversions to Metric Measures

Symbol	When You Know	Multiply by	To Find	Symbol
		LENGTH		
in	inches	*2.5	centimeters	cm
ft	feet	30	centimeters	cm
yd	yards	0.9	meters	m
mi	miles	1.6	kilometers	km
		AREA		
in^2	square inches	6.5	square centimeters	cm^2
ft^2	square feet	0.09	square meters	m^2
yd^2	square yards	0.8	square meters	m^2
mi^2	square miles	2.6	square kilometers	km^2
	acres	0.4	hectares	ha
		MASS (weight)		
oz	ounces	28	grams	g
lb	pounds	0.45	kilograms	kg
	short tons (2,000 lb)	0.9	tonnes	t
		VOLUME		
tsp	teaspoons	5	milliliters	ml
Tbsp	tablespoons	15	milliliters	ml
fl oz	fluid ounces	30	milliliters	ml
c	cups	0.24	liters	l
pt	pints	0.47	liters	l
qt	quarts	0.95	liters	l
gal	gallons	3.8	liters	l
ft^3	cubic feet	0.03	cubic meters	m^3
yd^3	cubic yards	0.76	cubic meters	m^3
		TEMPERATURE (exact)		
°F	Fahrenheit temperature	5/9 (after subtracting 32)	Celsius temperature	°C

*1 in = 2.54 (exactly). For other exact conversions and more detailed tables, see NBS Misc. Publ. 286, Units of Weights and Measures, Price $2.25, SD Catalog No. C13.10:286.

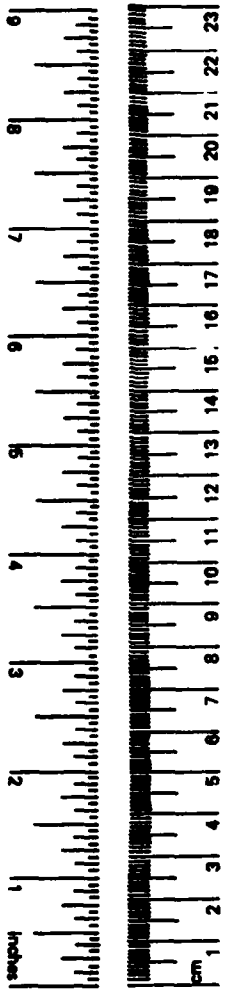

Approximate Conversions from Metric Measures

Symbol	When You Know	Multiply by	To Find	Symbol
		LENGTH		
mm	millimeters	0.04	inches	in
cm	centimeters	0.4	inches	in
m	meters	3.3	feet	ft
m	meters	1.1	yards	yd
km	kilometers	0.6	miles	mi
		AREA		
cm^2	square centimeters	0.16	square inches	in^2
m^2	square meters	1.2	square yards	yd^2
km^2	square kilometers	0.4	square miles	mi^2
ha	hectares (10,000 m^2)	2.5	acres	
		MASS (weight)		
g	grams	0.035	ounces	oz
kg	kilograms	2.2	pounds	lb
t	tonnes (1,000 kg)	1.1	short tons	
		VOLUME		
ml	milliliters	0.03	fluid ounces	fl oz
l	liters	2.1	pints	pt
l	liters	1.06	quarts	qt
l	liters	0.26	gallons	gal
m^3	cubic meters	35	cubic feet	ft^3
m^3	cubic meters	1.3	cubic yards	yd^3
		TEMPERATURE (exact)		
°C	Celsius temperature	9/5 (then add 32)	Fahrenheit temperature	°F

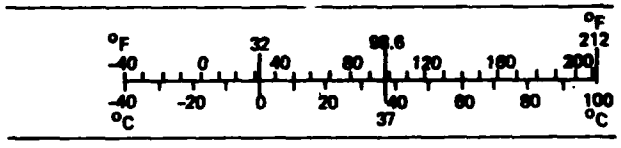

Unclassified

SECURITY CLASSIFICATION OF THIS PAGE (When Data Entered)

REPORT DOCUMENTATION PAGE		READ INSTRUCTIONS BEFORE COMPLETING FORM
1 REPORT NUMBER TN-1730	2 GOVT ACCESSION NO. DN487266	3 RECIPIENT'S CATALOG NUMBER AD-A163 563
4 TITLE (and Subtitle) A RECURSIVE BOUNDARY ELEMENT WITH INITIAL ERROR INVESTIGATION		5 TYPE OF REPORT & PERIOD COVERED Final; Oct 1984 – Sep 1985 6 PERFORMING ORG. REPORT NUMBER
7 AUTHOR(s) J. V. Cox and T. A. Shugar		8 CONTRACT OR GRANT NUMBER(s)
9 PERFORMING ORGANIZATION NAME AND ADDRESS NAVAL CIVIL ENGINEERING LABORATORY Port Hueneme, California 93043		10 PROGRAM ELEMENT, PROJECT, TASK AREA & WORK UNIT NUMBERS 61153N; YR023.03.01.005
11 CONTROLLING OFFICE NAME AND ADDRESS Naval Facilities Engineering Command Alexandria, Virginia 22332		12 REPORT DATE December 1985 13 NUMBER OF PAGES 43
14 MONITORING AGENCY NAME & ADDRESS(if different from Controlling Office)		15 SECURITY CLASS (of this report) Unclassified 15a DECLASSIFICATION DOWNGRADING SCHEDULE

16 DISTRIBUTION STATEMENT (of this Report)

Approved for public release; distribution unlimited.

17 DISTRIBUTION STATEMENT (of the abstract entered in Block 20, if different from Report)

18 SUPPLEMENTARY NOTES

19 KEY WORDS (Continue on reverse side if necessary and identify by block number)

Boundary element, ~~BEM~~, elastostatics, recursion, isoparametric numerical integration.

20 ABSTRACT (Continue on reverse side if necessary and identify by block number)

A recursive numerical integration technique is developed for the boundary element method. The initial implementation is within an indirect formulation for two-dimensional elastostatics. A numerical study investigates the error field near a single boundary element in the infinite plane using different orders of numerical integration. The difficulty of integrating the singular kernal functions with discrete integration points is eliminated with a recursive algorithm that adaptively subdivides elements that are in close proximity to the internal

continued

DD FORM 1 JAN 73 1473 EDITION OF 1 NOV 65 IS OBSOLETE

Unclassified

SECURITY CLASSIFICATION OF THIS PAGE (When Data Entered)

20. Continued

response point. The recursive technique allows calculation of internal responses arbitrarily close to the boundary with no loss of accuracy. This frees the analyst to design the boundary subdivision based on boundary geometry and anticipated boundary response gradients without regard for the numerical integration accuracy of responses near the boundary. The gradient of the artificial tractions must ordinarily be considered when modeling problems with the indirect formulation.

Library Card

Naval Civil Engineering Laboratory
A RECURSIVE BOUNDARY ELEMENT WITH INITIAL ERROR INVESTIGATION, by J. V. Cox and T. A. Shugar
TN-1730 43 pp illus December 1985 Unclassified

1. Boundary element 2. Elastostatics I. YR023.03.01.005

A recursive numerical integration technique is developed for the boundary element method. The initial implementration is within an indirect formulation for two-dimensional elastostatics. A numerical study investigates the error field near a single boundary element in the infinite plane using different orders of numerical integration. The difficulty of integrating the singular kernal functions with discrete integration points is eliminated with a recursive algorithm that adaptively subdivides elements that are in close proximity to the internal response point. The recursive technique allows calculation of internal responses arbitrarily close to the boundary with no loss of accuracy. This frees the analyst to design the boundary subdivision based on boundary geometry and anticipated boundary response gradients without regard for the numerical integration accuracy of responses near the boundary. The gradient of the artificial tractions must ordinarily be considered when modeling problems with the indirect formulation.

CONTENTS

INTRODUCTION

Boundary element methods (BEM) have become an accepted alternative to domain-based methods (finite element and finite difference) for many classes of boundary value problems. The direct and indirect BEM formulations are two reasonably established formulations that are used to solve a variety of boundary value problems in engineering. These methods require only the boundary to be subdivided and are inherently suitable when modeling infinite domains. Since the methods are relatively new, they have not been as extensively developed as domain methods for nonlinear applications. They also lack the generality (in terms of extensive continuum and structural element libraries) that commercial finite element method (FEM) computer programs possess.

Considering the individual strengths of domain- and boundary-based methods, some classes of problems (e.g., nonlinear soil-structure interaction) may be most effectively solved by combining the methods.

Objective

The ultimate objective of this research is to determine whether or not the boundary element and finite element solution methods can be combined with advantage towards economical solutions of nonlinear structural/geotechnical problems. However, our immediate emphasis is on improving the accuracy of the indirect boundary element method. The accuracy of a quadratic isoparametric boundary element with a new adaptive integration technique is evaluated.

Background

An early application of the direct method for elasticity is given by Cruse and Rizzo (Ref 1). In this formulation Betti's theorem is used to transform a volume integral to a surface integral. The unknown

boundary values for traction and displacements are solved for directly in the system of equations. Internal responses (stresses, strains, or displacements) are obtained as integrals of the tractions and displacements on the boundary of the domain.

An early application of the indirect method for elasticity is given by Massonnet (Ref 2). In the indirect formulation the actual boundary value problem is replaced by an auxiliary problem in the infinite plane (two-dimensional), and artificial boundary tractions that satisfy the boundary conditions and the governing differential equations constituting the actual problem are solved. These artificial tractions are then integrated to obtain internal and boundary responses of the actual problem.

Early efforts used analytically integrated elements with constant or linear interpolation of boundary variables. Lachat and Watson (Ref 3) incorporated isoparametric element representations typical of the finite element method (Ref 4). Geometry as well as boundary values could be interpolated at a consistent order (linear, quadratic, or cubic) over a given element.

Isoparametric representations prevent closed-form integration over individual elements and numerical integration is required. These element integrations represent the main computational effort of the BEM. Thus, there has been much effort aimed at efficient numerical integration (Ref 5, 6, and 7). Lachat and Watson (Ref 5) present a variable-order numerical integration strategy with provisions for element subdivision when the required order of integration, for a prescribed accuracy, exceeds that available in the program.

A Naval Civil Engineering Laboratory (NCEL) study of the BEM (Ref 8) compared the direct and indirect methods in two dimensional elastostatics with constant distribution elements. The direct method performed poorly (as compared to the indirect method) in a region near the boundary but gave good values on the boundary. This poor performance in the near boundary region was due to two factors: (1) the direct method computer code calculated the element integrations with four-point Gauss quadrature as compared to the indirect method computer code, which contained closedform integration formulas; and (2) internal response calculations in the

direct method must integrate a function with a higher order singularity. Based on the performance comparison of that study and the fact that the indirect method is less formal theoretically and simpler to physically comprehend, the indirect method was pursued further.

A following study (Ref 9) investigated a preliminary coupling of the finite element and boundary element methods in two-dimensional elastostatics. The methods were coupled within the computational framework of the BEM, satisfying compatibility and equilibrium explicitly at the domain interfaces. Qualitatively the coupling was a success, but the simple constant elements used for both methods prevented substantial quantitative evaluation. Coupling the two methods conceptually as two BEM domains provided a good initial study but was not as applicable to the long-term goals for application in nonlinear soil-structure interaction because the approach yielded a system of unsymmetric algebraic equations. Two areas, therefore, required further investigation: (1) accuracy of the BEM formulation, and (2) a FEM-BEM coupling within a FEM computational framework.

Scope

The present study addresses the accuracy of the indirect BEM. The main focus of the study is a new algorithm based on a recursive subdivision of boundary elements that improves the accuracy of isoparametric element integrations in the near-boundary region. Numerical integration error is studied in the context of the error field near a single boundary element in an infinite plane. Based on this numerical study, a criterion for element subdivision is determined as a function of desired accuracy. The recursive algorithm is presented along with some initial numerical examples to illustrate its effectiveness. Also included are the refinement of a variable-order integration formula, which is commonly used in boundary element work, and an investigation of numerical error that is characteristic of the indirect BEM near boundary discontinuities.

In addition to numerical integration error, the indirect boundary element method possesses error that is traceable to its inherent use of artificial boundary tractions. The actual boundary responses (tractions

or displacements) may have small gradients, while the corresponding artificial boundary tractions may have very high gradients. Thus, a boundary subdivision that appears sufficiently adequate for the boundary response can fail to accurately model the artificial tractions and thereby result in poor accuracy for internal response calculations. These errors occur near geometry and traction boundary discontinuities. One numerical example presented includes a study of this error as well as the error from numerical integration.

The computational aspects of this study were carried out on a microcomputer. The main incentives for this approach were limitation of cost and the availability at NCEL of an effective software development environment (the University of California at San Diego (UCSD) p-System) and a modern language (UCSD Pascal). Our use of a modern language has led us to pursue approaches such as the use of recursive constructs that would not have been considered in a FORTRAN environment. Strongly data-typed languages such as Pascal can generally provide a good research environment because of their enhanced data structures, internal documentation, and modularity.

Our recursive algorithm is implemented for the indirect BEM and with a quadratic isoparametric boundary element. The concepts underlying the indirect formulation are reviewed in the following section.

INTEGRAL EQUATIONS

The applicable integral equations are given here for reference and perspective. Detailed accounts of the integral equation development are given by Banerjee and Butterfield (Ref 10) and Crouch and Starfield (Ref 11). The equations given in the following section closely follow those given by Banerjee and Butterfield (Ref 10). Body forces and rigid body translations are omitted for brevity.

Both the direct BEM and indirect BEM are formulated in terms of the fundamental singular solution, the Kelvin solution for linear, isotropic, plane strain conditions, which expresses the displacement field $u_i(x)$ due to a unit force $e_k(\xi)$. The indices i, j, and k assume values of 1

or 2, and repeated indices imply summation in what follows. The Cartesian coordinates x and ξ represent the field and source points, respectively. The Kelvin solution is given by

$$u_i(x) = G_{ik}(x,\xi)\, e_k(\xi) \tag{1a}$$

where

$$G_{ik}(x,\xi) = C_1\left(C_2\, \delta_{ik} \ln r - \frac{y_i\, y_k}{r^2}\right) + A_{ik} \tag{1b}$$

$$C_1 = -\frac{1}{8\pi\mu(1 - \nu)}$$

$$C_2 = 3 - 4\nu$$

A_{ik} = arbitrary constant tensor based on zero displacement reference distance

$$y_i = x_i - \xi_i$$

δ_{ik} = Kronecker delta function

$$r^2 = y_i\, y_i$$

By incorporating the linear strain-displacement relationship and Hooke's law, the stress field $\sigma_{ij}(x)$ is given as

$$\sigma_{ij}(x) = T_{ijk}(x,\xi)\, e_k(\xi) \tag{2a}$$

where

$$T_{ijk}(x,\xi) = \left(\frac{C_3}{r^2}\right)\left[C_4(\delta_{ik}y_j + \delta_{jk}y_i - \delta_{ij}y_k) + \frac{2y_i y_j y_k}{r^2}\right] \tag{2b}$$

$$C_3 = -\frac{1}{4\pi(1 - \nu)} \tag{2c}$$

$$C_4 = 1 - 2\nu \tag{2d}$$

Equilibrium conditions applied at a boundary point, indicated by a unit outward normal $n_i(x)$, and Equation 2a combine to give the surface tractions $t_i(x)$ as

$$t_i(x) = F_{ik}(x,\xi)\, e_k(\xi) \tag{3a}$$

where

$$F_{ik} = \left(\frac{C_3}{r^2}\right)\left[C_4(n_k y_i - n_i y_k) + \left(C_4\,\delta_{ik} + \frac{2y_i y_k}{r^2}\right) y_j n_j\right] \tag{3b}$$

Figures 1 and 2 illustrate the singular behavior of the fundamental solutions G_{11} and T_{111}, respectively, for a point load applied at the origin of the Cartesian system. The singularity of G is order ln(r), while the singularity of T, obtained from derivatives of G, is order 1/r.

Consider the elastostatic boundary value problem shown in Figure 3 for a linear, isotropic, homogeneous domain Ω subjected to the traction and displacement boundary conditions:

$$t_i(x) = \hat{t}_i(x) \qquad \text{on } \Gamma_t \tag{4a}$$

$$u_i(x) = \hat{u}_i(x) \qquad \text{on } \Gamma_u \tag{4b}$$

where $\hat{t}_i(x)$ and $\hat{u}_i(x)$ are prescribed distributions of boundary tractions and displacements, respectively. The boundary conditions are not mutually exclusive; any two of the four boundary values are prescribed in a piecewise continuous manner for a well-posed problem. Boundary values can be defined in any orthogonal coordinate system and are not necessarily limited to the global x_1x_2 system.

When using the indirect BEM, the domain Ω is embedded in an infinite plane as shown in Figure 3.* Artificial tractions, $P_k(\xi)$, acting on the boundary Γ are sought that satisfy the prescribed boundary conditions. The artificial tractions can be expressed as a "continuous" distribution

*The plane strain formulation can be converted to the plane stress formulation by specifying an effective Poisson ratio $\nu = \nu/(1 + \nu)$.

of unknown point loads analogous to $e_k(\xi)$ and related to field variables by Equations 1 through 3. The displacements and stresses for any point x due to the artificial tractions are then given by integrals over the boundary

$$u_i(x) = \int_\Gamma G_{ik}(x,\xi)\ P_k(\xi)\ d\xi \qquad (\xi\ \varepsilon\ \Gamma) \tag{5}$$

$$\sigma_{ij}(x) = \int_\Gamma T_{ijk}(x,\xi)\ P_k(\xi)\ d\xi \tag{6}$$

The governing differential equations are satisfied over the entire plane including the domain Ω, since the responses are expressed as a superposition of the fundamental solution. From Equations 3a and 3b the tractions acting on a tangent line defined by a normal vector n_i are given by

$$t_i(x) = \int_\Gamma F_{ik}(x,\xi)\ P_k(\xi)\ d\xi \tag{7}$$

If the field point x is now allowed to approach the boundary Γ and the boundary conditions, Equations 4a and 4b, are enforced, we obtain boundary integral equations relating the known boundary values in terms of the unknown artificial boundary tractions as follows,

$$\hat{t}_i(x) = \int_\Gamma F_{ik}(x,\xi)\ P_k(\xi)\ d\xi \qquad \text{on } \Gamma_t \tag{8}$$

$$\hat{u}_i(x) = \int_\Gamma G_{ik}(x,\xi)\ P_k(\xi)\ d\xi \qquad \text{on } \Gamma_u \tag{9}$$

Equation 8 must be interpreted as a Cauchy principal value integral and is thus written as

$$\hat{t}_i(x) = \pm \frac{1}{2}\,\delta_{ik}P_k(x) + \int_\Gamma F_{ik}(x,\xi)\ P_k(\xi)\ d\xi \qquad \text{on } \Gamma_t \tag{10}$$

assuming a tangent line through x.

NUMERICAL FORMULATION

Equations 9 and 10 represent an exact boundary integral equation formulation of the problem of determining artificial tractions. Practical engineering methods require that the equations be solved numerically. Two numerical approximations are made:

(1) The boundary integrations are performed in a piecewise manner over discrete subdivisions of the boundary called boundary elements. Within each element tractions (real and artificial), displacements, and geometry are usually interpolated by polynomial functions.

(2) Equations 9 and 10 are satisfied at discrete points within each element by the collocation method. This can be considered as a weighted residual method with Dirac delta weighting functions having origins placed at the collocation points, i.e., points where the equations are exactly satisfied.

The integral equations can thus be approximated by a set of linear, simultaneous algebraic equations.

First consider the piecewise integration over the boundary. If the boundary is divided into Q boundary elements, the displacement at a response point x is given as

$$u_i(x) = \sum_{q=1}^{Q} \int_{\Delta\Gamma^q} G_{ik}(x,\xi)\, P_k(\xi)\, d\xi \qquad (11)$$

In an isoparametric element formulation any field variable γ (e.g., representing boundary geometry, traction, or displacement) defined on an element q can be interpolated in terms of nodal values and shape functions (Ref 5) as follows

$$\gamma_i = \sum_{\alpha=1}^{M} N_\alpha(\eta)\, \gamma_{i\alpha} \qquad (12)$$

where α is the node index, M is the number of nodes per element, η is the normalized ($-1 \leq \eta \leq 1$) local curvilinear coordinate, $y_{i\alpha}$ are nodal values of the field variable, and $N_\alpha(\eta)$ are the appropriate polynomial shape functions for the element. A quadratic element (M=3) is shown in Figure 4. The shape functions for this element are defined as

$$N_1 = \frac{1}{2}(\eta^2 - \eta) \tag{13a}$$

$$N_2 = (1 - \eta^2) \tag{13b}$$

$$N_3 = \frac{1}{2}(\eta^2 + \eta) \tag{13c}$$

By interpolating the distribution of artificial tractions on element q, P^q_k, with Equation 12, the displacement at point x can be written as*

$$u_i(x) = \sum_{q=1}^{Q} \sum_{\alpha=1}^{M} P^q_{k\alpha} \int_{-1}^{1} G^q_{ik} N_\alpha J^q \, d\eta \tag{14}$$

where J^q is the Jacobian relating the global Cartesian system ξ to the local curvilinear system η. The Jacobian is given by

$$J^q = \left[\left(\frac{\partial \xi_1}{\partial \eta} \right)^2 + \left(\frac{\partial \xi_2}{\partial \eta} \right)^2 \right]^{1/2} \tag{15}$$

It is a function of η, and its value is an indicator of the geometric distortion of the qth boundary element. Introduction of the shape functions allows the unknown nodal values of artificial traction $P^q_{k\alpha}$ to be removed from the integrand as constant coefficients of the integral.

An expression for the stress and traction at any point x can be written in a similar manner as follows

*The superscript q is not to be interpreted as an exponent.

$$\sigma_{ij}(x) = \sum_{q=1}^{Q} \sum_{\alpha=1}^{M} P_{k\alpha}^{q} \int_{-1}^{1} T_{ijk}^{q} N_{\alpha} J^{q} \, d\eta \qquad (16)$$

$$t_{i}(x) = \sum_{q=1}^{Q} \sum_{\alpha=1}^{M} P_{k\alpha}^{q} \int_{-1}^{1} F_{ik}^{q} N_{\alpha} J^{q} \, d\eta \qquad (17)$$

Equations 14 and 17 can be applied at collocation points on the boundary to obtain an approximate solution to Equations 9 and 10. For isoparametric elements the number of element collocation points is equal to the number of nodal points. The collocation points can be positioned at the geometric node points giving continuous elements, or the points can be positioned within the element giving discontinuous or nonconforming elements (Ref 12). The known boundary values are interpolated at the collocation points, thus giving a system of algebraic equations in terms of the unknown tractions $P_{k\alpha}^{q}$. After having solved this system for $P_{k\alpha}^{q}$, the displacement and stress response in the domain Ω or on the boundary Γ can be obtained by applying Equations 14 and 16, respectively.

The element integrations of Equations 14, 16, and 17 constitute the main computational effort of the indirect boundary element method for linear elastostatic problems and are the focus of this study.

ELEMENT INTEGRATION

Except when using simple elements, numerical integration is generally a necessary part of the procedure for calculating the system of equations and internal responses in the BEM. In developing the system of equations, when the collocation point is on the boundary element to be integrated the integration must receive special treatment. These integrations over the singularity are treated in detail by Watson (Ref 13) and by Banerjee and Butterfield (Ref 10). A combination of analytical and numerical integration is usually required.

The element integrations for internal response calculations can also require special treatment. We will concentrate on the evaluation of stress because it is associated with a stronger singularity than displacement (compare Figures 1 and 2). One approach to the integration is the single application of Gaussian-Legendre numerical integration (Ref 14). For a given function $k(\eta)$, its integral is numerically evaluated as

$$\int_{-1}^{1} k(\eta)\, d\eta = \sum_{i=1}^{\bar{M}} A_i\, k(\eta_i) \qquad (18)$$

where A_i and η_i are the integration weights and positions (Gauss points), respectively, for integration order $\bar{M}$. In the indirect BEM this represents the replacement of a continuous traction with a distribution of discrete forces at positions η_i. The stress field is thus given by the superposition of singular fields of the type shown in Figure 2 with origin placed at each integration point η_i and with corresponding weight factor A_i.

The accuracy of element integrations can be examined experimentally in the context of a single element in the infinite plane, as shown in Figure 5. Figure 5 also depicts the response region and view direction for graphical results presented in Figures 6, 7, and 8. Figures 6a, 7a, and 8a show the stress (σ_{11}) field in the response region using various orders of numerical integration. Four-point integration is typically used in codes where the order of integration is not designed to vary. The singular behavior at the Gauss points is clearly evident. As the element (which lies along the line x=0) is approached the stress and thus the error become unbounded near a Gauss point. The error in numerical integration can be evaluated by comparing the results with those obtained from an analytically integrated constant element. The σ_{11} error field for various orders of integration is shown in Figures 6b, 7b, and 8b. A positive value indicates an overestimate of the compressive stress magnitude. The error plots are arbitrarily clipped at ±2%. The variation in weight factors, A_i, for the integration points are reflected in the variation in the peaks on all the figures. At half an element length or

greater away from the traction, the stress σ_{11} for four-point integration has an error of less than 0.6% (Figure 6b). At this distance the stress is adequately computed by four-point quadrature. The region closer to the element is herein referred to as the "error region." The size of this region is dependent on the acceptable error level. The oscillation observed in the response has been referred to as the ripple effect in previous reports (Ref 15 and 8).

There are different approaches to improving the accuracy in the error region. Some approaches reduce the size of the error region, while others avoid using the boundary integration to calculate responses in the error region. Increasing the order of numerical integration reduces the weight factors A_i and the distance between individual Gauss points, thus reducing the size of the error region. This has been illustrated in Figures 7 and 8, which give the stress and error fields using 8- and 16-point numerical integration, respectively. The error region is sigificantly reduced. Other approaches for reducing the error region include element subdivision and analytical integration of extracted portions of the integrand. The element subdivision approach involves subdividing the element and performing the integrations over smaller segments of the element. Alternatively, shape functions can be used to interpolate through the error region (bridge the region), since boundary values for points exactly on the boundary are obtained accurately.

When accuracy requirements exceed the order of integration that is available in the program (i.e., when the response point is within the error region of a given element), one of the previously mentioned remedies may be used. Interpolation through the error region can give good results, but it can also constrain the choice of the element size if the analyst is also anticipating a need for calculating near-boundary response points. From the analyst's perspective it would be more appropriate to base the selection of element size only on considerations of geometry and anticipated response gradients along the boundary. In this regard, an element subdivision approach is attractive since it obviates the need for apriori consideration of near-boundary response point calculations when designing the boundary discretization.

The variation in size of the error region with order of numerical integration suggests that the order of integration be determined as a function of normalized distance to the element $\bar{r}$; where $\bar{r}$ is the ratio of the distance between the field point and the element, r, to the element length, $\Delta\ell$. Other factors include the element distortion, traction distribution, and the position of the response point relative to the element.

In this study the order of integration is adaptively selected for each combination of element and field point. It is given by a procedure that includes $\bar{r}$ and a user-specified error parameter, based on work originally done by Lachat and Watson (Ref 5). The actual formula used to select the order of integration ($\bar{M}$) is a modification of one given by Banerjee and Butterfield (Ref 10).

The variation of $\bar{M}$ given by Banerjee and Butterfield's formula, for three different (user-defined) error thresholds, is shown in Figure 9. For each error threshold the order of integration increases as $\bar{r}$ decreases until $\bar{M}$ unexpectedly decreases very near the element. The decrease in order near the element is a mistake that can cause less reliability in the near-boundary region. Some implementations will "key" on $\bar{M}$ to determine if element subdivision is necessary; this formula would then result in no element subdivision where it is needed most. Other strategies for refining the results in the near-boundary region would not be affected by the behavior of Banerjee and Butterfield's formula.

A revised version of the formula is given below in a Pascal-like outline.

```
PROCEDURE ORDERcalc

CONSTANTS
     ZEROtolerance:= -2.0E-3;
     GAUSSINTmax:= 16;

BEGIN (* the ORDERcalc procedure *)
LNERRORover8:= LN(ERRORparameter/8)
LNLover4R:= LN(LENGTH*0.25/RADIUSmin)
IF LNLover4R>ZEROTOL THEN LNLover4R:= ZEROTOL
ORDER:= ROUND(0.5*ABS(LNERRORover8/LNLover4R-1.0)) + 1
IF ORDER>GAUSSINTmax THEN ORDER:= GAUSSINTmax
END  (* the ORDERcalc procedure *)
```

The variation of $\bar{M}$ given by this formula, for three different error parameters, is shown in Figure 10. The revision gives the formula an asymptotic behavior as the element is approached. In the research software developed for this study (Single Element Integration Tester (SEIT) and BEM Quadratic Element TEST (BQTEST)), the order of integration could vary from 1 to 16. The formula merits further investigation. Though it is a simple formula it can drastically affect the efficiency and accuracy of the method. The SEIT program could readily be used to fit a curve to the numerical error data.

Practical limitations to increasing the order of numerical integration can arise, especially in the context of the direct boundary element method, where the singularity for stress integrations is more severe than in the indirect method ($1/r$ versus $1/r^2$).

The element subdivision algorithm developed here recursively subdivides the element. It is implemented in an adaptive manner and results in a concentration of subelements near the response point of interest. The use of recursion allows a general algorithm that is otherwise difficult to implement for curved elements when based on an alternative iterative approach. The adaptive concentration of subelements in the proximity of the response point helps minimize the number of integration points. The following section gives an overview of the algorithm followed by a more detailed pseudo-code (an outline of an algorithm written in a combination of English and computer programming language).

RECURSIVE QUADRATIC ELEMENT

Consider the isoparametric quadratic element shown in Figure 11. Based on experiments illustrated in the previous section a constant ratio $\bar{r}_{sub}$ can be established that bounds the element error region as shown by the dashed line. In our studies, for example, for order 16 integration, responses have less than 0.1% error for values of $\bar{r} > 0.2$. This value is obtained for an element with both a constant traction distribution and a constant Jacobian. The criterion that the radius must satisfy to avoid subdivision of the element is given by

$$r > \Delta\ell \; \bar{r}_{sub} \tag{19}$$

Element subdivision must be used to obtain consistent accuracy for response points inside of this radius.

The radius r can be estimated by calculating the distance to the nearest node point when the interior response point position, x_i^p, is relatively far from the element (e.g., $r > \Delta\ell$). When close to the element the radius r may be considered as a continuous function of the local coordinate η. The minimum radius to the element can then be calculated by minimizing the square of the radius with respect to η.*

The closest point on the element is indicated by local coordinate η_0 in Figure 11a and is the focal point for the initial element subdivision. A "critical" element $\Delta\Gamma^{cr}$ is centered at $x_i(\eta_0)$ as shown in Figure 11b with a length of $\Delta\ell^{cr}$ given by

$$\Delta\ell^{cr}(\xi) = \frac{r}{\bar{r}_{sub}} \tag{20}$$

Assuming a constant Jacobian over the subelement, the length in the local coordinate is given as

$$\Delta\eta^{cr} = \frac{\Delta\ell^{cr}(\xi)}{J(\eta_0)} \tag{21}$$

The inaccuracy introduced by the assumption of a constant Jacobian can be overcome if the user-specified ratio $\bar{r}_{sub}$ is set slightly greater than the value computed based on this assumption (e.g., 0.3 instead of 0.2 in this case). This can result in more subdivision since $\Delta\ell^{cr}$ will

*The possibility of obtaining two minimum radius values poses no problem to the recursive procedure.

be smaller, but the inclusion of variable-order integration will reduce the order of numerical integration on the individual subelements if the specified ratio $\bar{r}_{sub}$ is overly conservative.

The element integrations can now be performed with consistent accuracy over $\Delta\Gamma^{cr}$ with respect to the subelement local coordinate η^{cr} and subelement shape functions $N_\beta(\eta^{cr})$. The contribution of subelement $\Delta\Gamma^{cr}$ in element q to the traction t_i^q, for example, at x_i^p is given by

$$\sum_{\alpha=1}^{M=3} P_{k\alpha}^q \sum_{\beta=1}^{M=3} N_{\alpha\beta} \int_{-1}^{1} F_{ik}^q \, N_\beta(\eta^{cr}) \, J \, d\eta^{cr} \qquad (22)$$

where $N_{\alpha\beta}$ is the value the αth element shape function at node β of the subelement. The quadratic element shape functions are thus being approximated by the quadratic subelement shape functions N_β. In a similar manner, integrations over the remainder of the element subregions $\Delta\Gamma^a$ and $\Delta\Gamma^b$ shown in Figure 11b can be incorporated into the original element integrations. Expression 22 is the key to subdivision algorithms, whether they are implemented with iterative or recursive algorithms.

The minimum radius criterion, Equation 19, is also applied to subregions $\Delta\Gamma^a$ and $\Delta\Gamma^b$. Subelement $\Delta\Gamma^{cr}$ explicitly satisfies the criterion by Equation 20. The remaining element subregions, in general, do not satisfy the subdivision criterion and must be further subdivided. A recursive application of the subdivision procedure described above can then be applied to the remaining element subregions. Figure 11c illustrates this process by subdividing $\Delta\Gamma^a$. Primes denote one level of recursion. The closest point on $\Delta\Gamma^a$ to the response point is at $\eta' = 1$. Since this is at the end of the subregion, the critical subelement is not centered on η_0', and further it is assumed that $\Delta\Gamma^{b'}$ in this case is not needed, (i.e., no further subdivision of $\Delta\Gamma^b$ is required). The critical subelement $\Delta\Gamma^{cr'}$ can now be integrated and incorporated into the integrals for the subregion $\Delta\Gamma^a$ shape functions using Expression 22. Assume now that $\Delta\Gamma^{a'}$ satisfies Equation 19 (i.e., no further subdivision is necessary for $\Delta\Gamma^a$). It can then be integrated and incorporated into the subelement integrations. With the integrations complete on $\Delta\Gamma^a$, Expression 22 incorporates contributions into the integration over $\Delta\Gamma$.

The integrations over the element $\Delta\Gamma$ using the original element shape functions have been completed except for the element subregion $\Delta\Gamma^b$. As indicated in Figure 11b, the length of $\Delta\Gamma^b$ is less than that of $\Delta\Gamma^{cr}$, while the radius r to $\Delta\Gamma^b$ is greater than that to $\Delta\Gamma^{cr}$; Equation 19 is satisfied. Thus, in this case $\Delta\Gamma^b$ would require no further subdivision. Subregion $\Delta\Gamma^b$ can be integrated and incorporated into the integrals for the element shape functions using Expression 22.

In software programming parlance, recursion is the ability of a function or subroutine to call itself. One strength of a recursive implementation, as contrasted with an iterative implementation, is that the element subdivision algorithm can directly deal with the case when the point η_0' is internal to $\Delta\Gamma^a$ (not at an extrema). This case can occur with curved elements. An iterative implementation of the subdivision procedure would require significant "bookkeeping" to monitor which portions of the element $\Delta\Gamma$ had been integrated. The recursive approach also yields compact code. Recursion, though a common feature in "modern computer languages" such as Pascal, Modula II, and C, is not a standard feature of FORTRAN. Pascal was the programming language used in this study.

An outline of the recursive element subdivision algorithm, written in pseudo-code, is given below. In this description in pseudo-code, Pascal procedure (analogous to a FORTRAN subroutine) calls of the element are either (1) replaced with a description of the procedure's actions or (2) explicitly shown with a listing of the procedure after the main element procedure QUAD. (A procedure call is not prefaced by the CALL statement as in FORTRAN.) Formal parameters of the procedures are not shown in Pascal syntax and are only included if they clarify the recursive nature of the algorithm. Comments that explain rather than replace code are enclosed within the delimiters (* and *).

```
PROCEDURE QUAD
   (INTEGRATIONS,    (* the element integration results *)
   Δℓ,               (* element length estimate *)
   x)                (* array of element nodal coordinates *)
```

```
PROCEDURE QUADnonsing
   (INTEGRATIONS, (* the element integration results *)
   Δℓ,            (* element length estimate *)
   x,             (* array of nodal coordinates *)
   r)             (* minimum radius to the field point *)


BEGIN (* the QUADnonsing procedure *)
Calculate the order of numerical integration (M̄) using the ORDERcalc
   procedure previously defined
Intialize the INTEGRATIONS array to zero
FOR i= 1 TO M̄ (* each integration point *)
  BEGIN (* the integration point loop *)
    For each of the element integrations (e.g., as in Equation 17)
      add the product of the integrand at the Gauss point with the
      Gauss weight to the appropriate INTEGRATIONS array value
  END (* the integration point loop *)
END (* the QUADnonsing procedure *)


BEGIN (* the QUAD procedure *)
Calculate the minimum radius (r) and the close point (η_o)
IF r>Δℓ*r̄_sub        (* subdivision criteria of Equation 19 *)
  THEN (* the element does NOT need to be subdivided *)
    QUADnonsing(INTEGRATIONS,Δℓ,x,r) (* integrate the entire element *)

  ELSE (* the element must be subdivided *)
    BEGIN
      Initialize the INTEGRATIONS values to zero
      Determine preliminary values for subelement integrations
        calculate Δℓ^cr by Equation 20
        calculate x^cr an array of the critical subelement nodal elements
      QUADnonsing(INTEGRATIONS^cr,Δℓ^cr,x^cr,r) (* integrate the critical
                                                   subelement *)
```

```
      Update the element integrations by Expression 22
      IF x^cr(η_1^cr)≠x(η_1) (* subelement node 1 does not coincide with
                              element node 1 *)
        THEN (* a Δr^a subelement is necessary *)
          BEGIN
            Interpolate the coordinates of x^a(2)
            Estimate the length Δℓ^a using two-point integration
            QUAD(INTEGRATIONS^a,Δℓ^a,x^a) (* a recursive call *)
            Update the element integrations as Expression 22
          END
      IF x^cr(η_3^cr)≠x(η_3) (* subelement node 3 does not conincide with
                              element node 3* )
        THEN (* a Δr^b subelement is necessary *)
          BEGIN
            Interpolate the coordinates of x^b(2)
            Estimate the length Δℓ^b using two-point integration
            QUAD(INTEGRATIONS^b,Δℓ^b,x^b) (* a recursive call *)
            Update the element integrations as Expression 22
          END
    END (* the element subdivision *)
END (* the QUAD procedure *)
```

The recursive procedure outlined above applies a variable-order integration formula at every level of recursion. The effect of the algorithm is to concentrate integration points on the boundary near the interior response point x_i^p. In this algorithm integration points further from x_i^p will increase in weight and spacing. This is consistent with the idea of variable-order integration applied around the problem boundary (Ref 5), but here it is applied at the element level.

The maximum order of integration available in the program is used in the determination of the error region. If the error region were to have been based on single-point integration, the recursive algorithm would use a "minimum" number of integration points adaptively positioned to account for the element distortion. Though the number of integration

points would be minimized, the number of recursive subdivisions would be maximized. Efficiency studies comparing these two factors are a future goal.

Each level of recursion has a corresponding amount of computational overhead. Subelement lengths and nodal positions, minimum distance r, integration order $\bar{M}$, and incorporation of the subelement integration results into the original integrals (Expression 22) are all calculations associated with a recursive subdivision. Each level of recursion also requires memory to accommodate the local variables and pointers to formal parameters passed to the recursive procedure (subroutine). For small values of $\bar{r}_{sub}$, the number of recursion levels required is small, even for response points very close to the element. For a constant Jacobian element with $\bar{r}_{sub} = 0.25$, the maximum number of levels of recursion for r = 0.01 and r = 0.001 is 2 and 3, respectively.

With the concepts of the recursive procedure explained, the actual accuracy of the recursive element is assessed in the next section.

NUMERICAL RESULTS

Consistent with the previous study of numerical integration error, the accuracy of the recursive element is first demonstrated for a single element in an infinite plane. Figure 12a presents the stress (σ_{11}) in the problem defined by Figure 5. Compare these results with those given by Figures 6 through 8. The recursive element removes the singularity behavior previously noted at the Gauss points. Figure 12b gives the percent error in the integration. Notice that with $\bar{r}_{sub} = 0.15$, there is a small amount of ripple present for $\bar{r} > 0.15$, the region in which subdivision is precluded. For $\bar{r} < 0.15$, the element adaptively subdivides the element and the error is virtually eliminated. If $\bar{r}_{sub}$ is increased to 0.30, the error is further reduced but at the cost of increased computational effort. If the radius (r) is simply computed using only the minimum nodal radius, the results, shown in Figure 13, are poor in the error region except near the nodes where the calculation method is valid. Between nodes, r is over estimated and thus the subdivision criterion of Equation 19 is mistakenly satisfied.

The recursive element is next demonstrated on two finite domain problems. The classic problem of a hole in a finite plate is demonstrated first. This test problem illustrates the accuracy that can be attained with the recursive element near the boundary even with high stress gradients present. The second test problem is a square plate subjected to uniform tension. This theoretically simple problem illustrates the difficulty the indirect BEM formulation has near geometric discontinuities. Also a parameter study was conducted to illustrate how the error field is affected by a collocation point location near the corner.

Figure 14 defines the stress concentration problem and indicates the region in which the internal response is calculated. Sixteen quadratic elements were used to model the boundary of the plate: eight for the square and eight for the circle. Discontinuous elements were used in the corners. The collocation points for the "corner nodes" only were positioned at $|\eta| = 0.80$. All other nodes that were common to two elements were continuous (i.e., the collocation points were placed at the geometric nodes).

In developing the system of equations, integrations over the singularities were avoided. The collocation points were positioned at a distance $r = 0.001\Delta\ell$ from the element inside the domain Ω. The mathematical limit was thereby replaced by a physical limit since the recursive element is designed to handle near-boundary responses. This is not necessarily the most computationally efficient means of calculating the integrations, but it is simple to implement and prevents further complication of the element integration procedure.

The calculation of internal responses is performed both with the simple four-point quadrature method and with the recursive technique. The response points are spaced at 0.06 in a square grid. Thus, the distance of the response points from the circular hole varies around the circumference. Figure 15 presents the stress (σ_{11}) near the hole using four-point quadrature. The ripple effect near the hole is quite prevalent. The same responses calculated with the recursive technique are given in Figure 16. The oscillation of the response near the hole is removed; thus, values in the high gradient regions of interest are accurately

predicted. At a distance of 0.001 from the top of the hole the stress concentration factor was 3.06. This compares well with theoretical solutions for an infinite plate, 3.00, and the finite plate, 3.04 (Ref 16). Error with respect to the finite plate solution (at the exact top of the hole) is 0.66%.

Figure 17 defines the uniaxial tension problem and indicates the region in which the internal response is calculated. The problem was modeled using both four and eight elements of uniform length. The collocation positions near the corner were varied to study the effect on the corner response. All collocation points were positioned within the domain to develop the system of equations (as explained in the previous test problem).

The results for the four- and eight-element models are shown in Figures 18 and 19, respectively. The nonrecursive integration results use the variable-order integration formula but are limited to a maximum integration order of 16. As with the previous problem the recursive element effectively eliminates the near-boundary error that is characteristic of the usual implementation of Gauss quadrature. The computed artificial boundary tractions for both models are sketched in Figure 20. The improvement in modeling these artificial tractions with an increase in the number of elements was apparent in the computed stress response of Figures 18b and 19b. In the previous test problem, responses were examined near a geometrically continuous portion of the boundary (the hole) so no severe gradients occur in the corresponding artificial tractions. However, in this test problem the responses approach the corner that has geometry and traction discontinuities and gradients are present in the corresponding artificial tractions. The error in the corner reflects an inherent weakness of the indirect boundary element formulation. The artificial boundary tractions become unbounded near the corner and are difficult to represent with polynomial element shape functions.

The positions of the corner collocation points and the element middle nodes (eight-element model) can be varied to improve the results without significantly affecting the cost of the analysis. The effect of shifting the middle nodes toward the corner would probably improve the

results since the middle node collocation point would be in a position to better model the gradient. The middle node position was not considered in this study. By similar reasoning, the position of the discontinuous corner node's collocation point is expected to affect the results. Figure 21 gives the error field in the domain for various positions of the corner collocation points. The error field for this problem is minimized when η 0.80. The error approaches zero near the collocation points where the boundary conditions are satisfied exactly. In addition to the difficulty of modeling the artificial tractions, collocation points positioned very close to the corner can result in equations that approach linear dependence and are numerically ill-conditioned.

CONCLUSIONS

A new recursive element subdivision algorithm is presented for the boundary element method. The algorithm is introduced within the context of the indirect boundary element method using an isoparametric quadratic element; it is, however, generally applicable to the direct boundary element method and other element formulations.

The motivation for this study and the resulting recursive algorithm development is to improve the reliability of the boundary element method by improving accuracy in the near-boundary region where error is normally excessive. As a result of the algorithm, the analyst can choose element size on the basis of geometry and anticipated response gradients alone without concern for avoiding the error in the internal response in the near-boundary region. This is similar to the idea behind the isoparametric element formulations in the finite element method, where fewer elements are necessary to capture geometric description while at the same time maintaining sufficient accuracy to model higher gradients.

In the indirect boundary element formulation the gradients of the artificial boundary tractions must be considered when subdividing the boundary. This is a practical limitation of the indirect method since these gradients are more difficult to identify on a physical basis. As

illustrated in this study, the artificial tractions can have very high gradients near geometric and loading discontinuities. Concentrating elements near the discontinuities is one way to capture these gradients.

The computational liability attending the new algorithm is the recursive subdivision of a few elements, but this is at least partially offset by a reduction of elements otherwise required in anticipation of near-boundary response point calculations.

The recursive algorithm is, on the basis of preliminary implementation, believed to be relatively simple to implement compared to an iterative approach that would also allow the same generality with curved elements. It also lends itself to surface elements for three-dimensional applications.

The adaptive quality of the recursive subdivision procedure potentially enhances the use of the method in computer-aided design (CAD) environments where the user may not have a complete understanding of the numerical behavior of the boundary element method in the near-boundary region. It would appear that it is also applicable to stress analysis applications in plasticity and fracture mechanics where response accuracy near the boundary is vitally important.

RECOMMENDATIONS

One of the objectives in our research has been a combined finite element and boundary element program that could reduce the high cost now associated with nonlinear finite element programs. Further work is needed for an effective coupling with nonlinear finite element programs. A boundary element formulation that produces a symmetric set of equations is essential. The concepts for an approach that produces a symmetric stiffness matrix were outlined in this year's effort. This approach would allow a much easier coupling of the BEM with existing FEM programs.

The recursive algorithm in this year's effort adaptively integrated the elements. The adaptive refinement of a combined FEM/BEM "mesh" could drastically increase the efficiency of this class of problems. The application of a recursive algorithm to adaptively refine a FEM/BEM mesh should be investigated.

The authors recommend that two areas receive further investigation: (1) a stiffness coupling of the BEM with the FEM, and (2) adaptive methods for combined boundary and finite elements.

REFERENCES

1. T.A. Cruse, and F.J. Rizzo. "A direct formulation and numerical solution of the general transient elasto-dynamic problem," Journal of Mathematical Analysis and Applications, vol 22, 1968, pp 244-259.

2. C.E. Massonnet. "Numerical use of integral procedures," in Stress Analysis, O.C. Zienkiewicz and G.S. Holister, editors. John Wiley and Sons, London, England, John Wiley and Sons, 1965, Chapter 10.

3. J.C. Lachat and J.O. Watson. "A second generation boundary integral equation program for three-dimensional elastic analysis," American Society of Mechanical Engineers Applied Mechanics Division National Conference, New York, 1975.

4. O.C. Zienkiewicz. The finite element method, third edition, London, England, McGraw-Hill, 1977.

5. J.C. Lachat and J.D. Watson. "Effective numerical treatment of boundary integral equations: A formulation for three-dimensional elastostatics," International Journal for Numerical Methods in Engineering, vol 10, 1 Jan 1976, pp 991-1005.

6. F.J. Rizzo and D.J. Shippy. "The boundary element method in thermo-elasticity," in Developments in Boundary Element Methods, P.K. Banerjee and R. Butterfield, editors. London, England, Applied Science Publishers, 1 Jan 1979, Chapter 7, pp 155-172.

7. L. Bolteus and O. Tullberg. "Bemstat - A new type of boundary element program for two-dimensional elasticity problems," in Boundary Element Methods, edited by C.A. Brebbia, Proceedings of the Third International Seminar, Irvine, Calif., Jul 1981. Berlin, Germany, Springer-Verlag, 1981, pp 518-537.

8. Naval Civil Engineering Laboratory. Technical Note N-1664: An investigation of the indirect boundary element method in one- and two-dimensional elastostatics, by T.A. Shugar and J.V. Cox. Port Hueneme, Calif., May 1983.

9. Naval Civil Engineering Laboratory. Technical Note N-1710: A study of coupling the boundary and finite element methods in two-dimensional elastostatics, by T.A. Shugar and J.V. Cox. Port Hueneme, Calif., Oct 1984.

10. P.K. Banerjee and R. Butterfield. Boundary element methods in engineering science. New York, N.Y., McGraw-Hill Book Company, 1981.

11. S.L. Crouch and A.M. Starfield. Boundary element methods in solid mechanics. Winchester, Mass., Allen S. Urwin Inc., 1983.

12. C. Patterson and M.A. Sheik. "Non-conforming boundary elements for stress analysis," in Boundary Element Methods, edited by C.A. Brebbia, Proceedings of the Third International Seminar, Irvine, Calif., Jul 1981. Berlin, Germany, Springer-Verlag, 1981, pp 137-152.

13. J.O. Watson. "Advanced implementation of boundary element method in two- and three-dimensional elastostatics," in Developments in Boundary Element Methods, P.K. Banerjee and R. Butterfield, editors. London, England, Applied Science Publishers, 1 Jan 1979, Chapter 3, pp 31-63.

14. A.H. Stroud and D. Secrest. Gaussian quadrature formulas. Englewood Cliffs, N.J., Prentice-Hall, 1966.

15. J.H. Bode. The solution of mixed boundary value problems in the theory of elasticity by a boundary integral equation technique, Ph D thesis, Michigan Technological University. Houghton, Mich., 1976.

16. R.J. Roark and W.C. Young. Formulas for stress and strain, Fifth edition. New York, N.Y., McGraw-Hill Book Company, 1975.

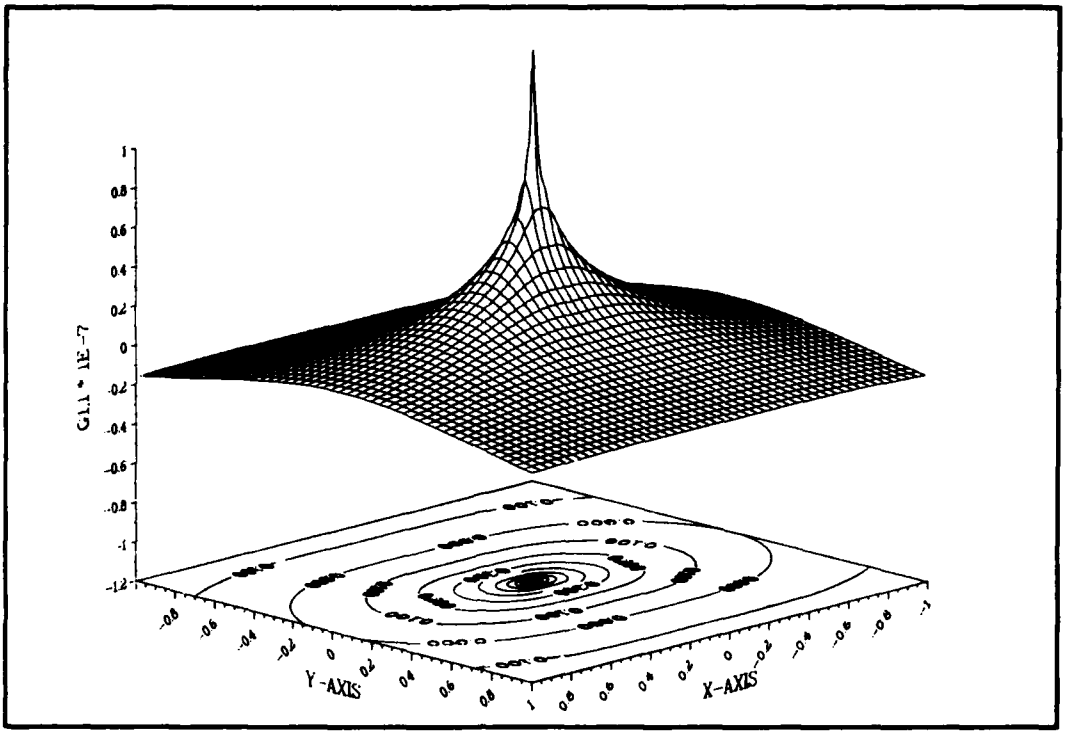

Figure 1. Displacement fundamental solution, G_{11}.

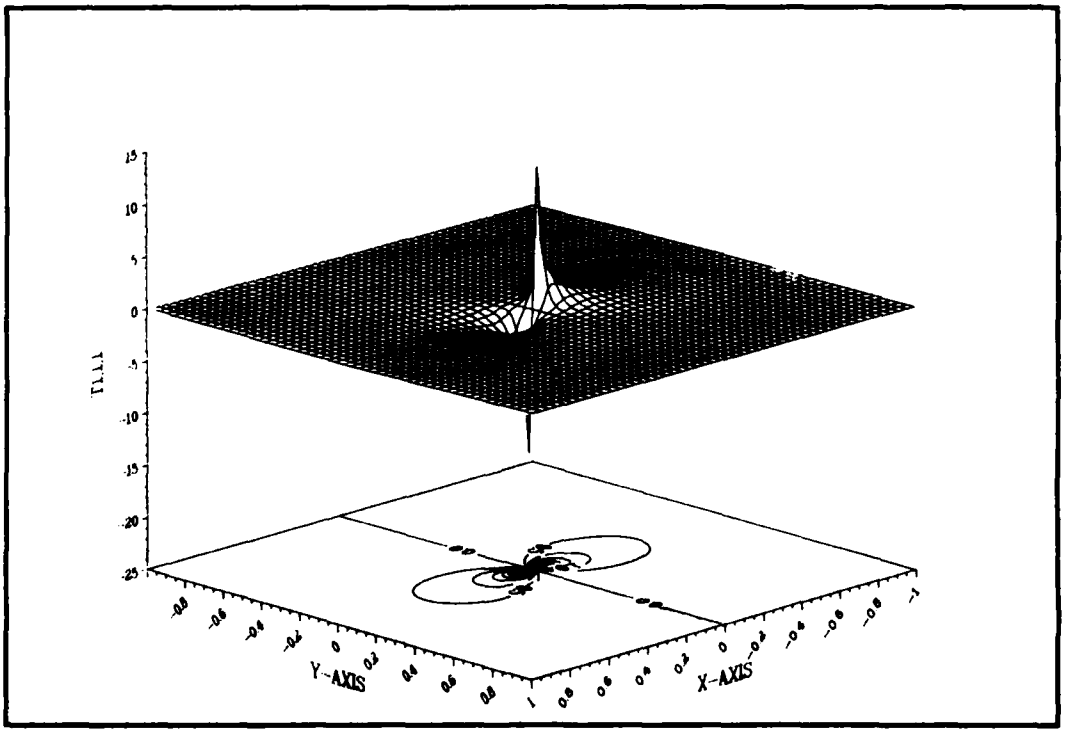

Figure 2. Stress fundamental solution, T_{111}.

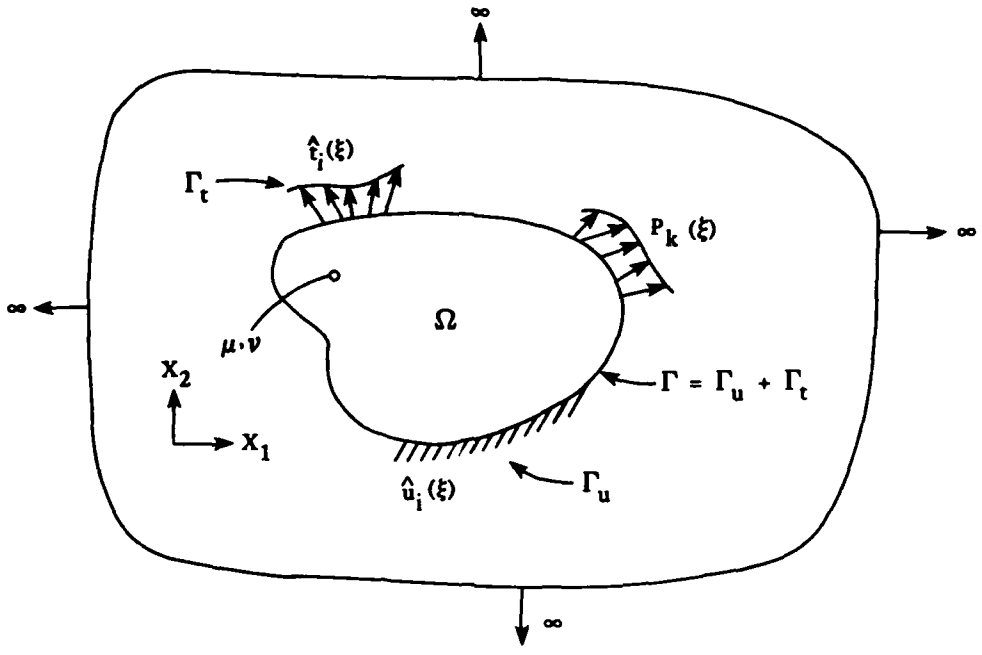

Figure 3. Two-dimensional elastostatics problem embedded in an infinite plane.

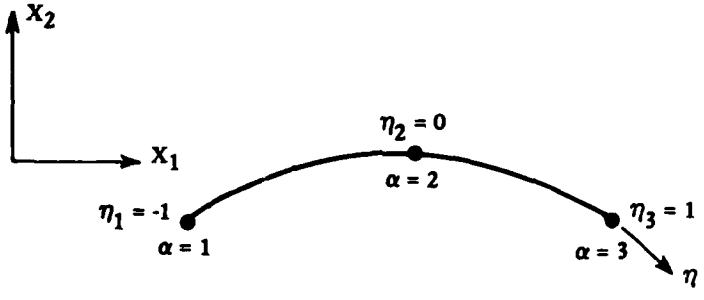

Figure 4. Quadratic isoparametric boundary element.

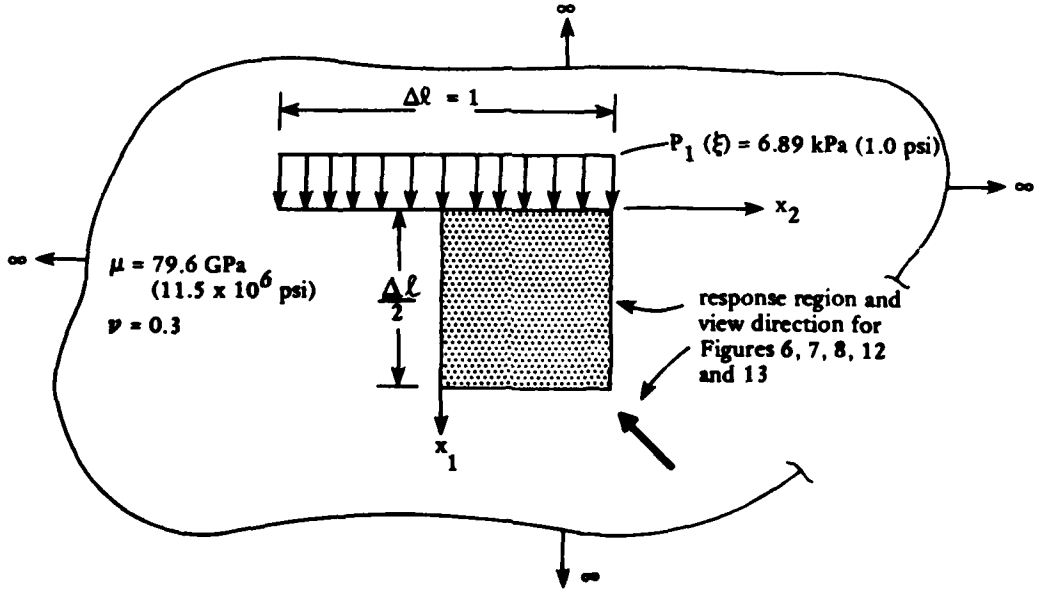

Figure 5. Uniform traction in an infinite plane.

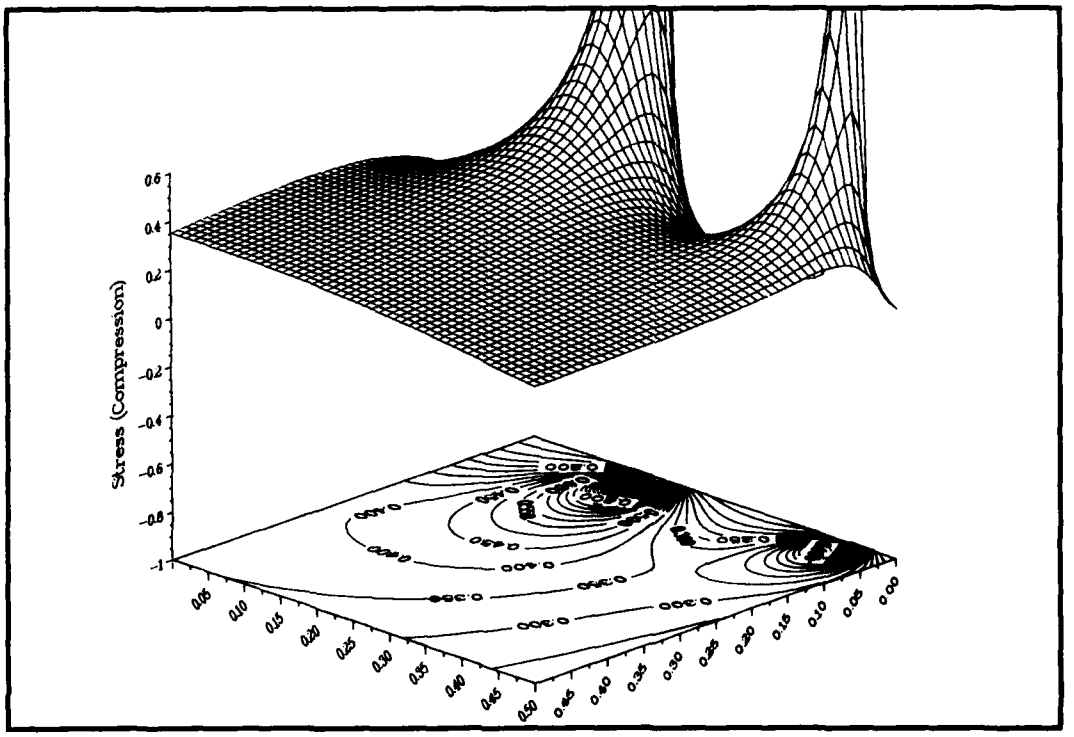

(a) σ_{11} stress field.

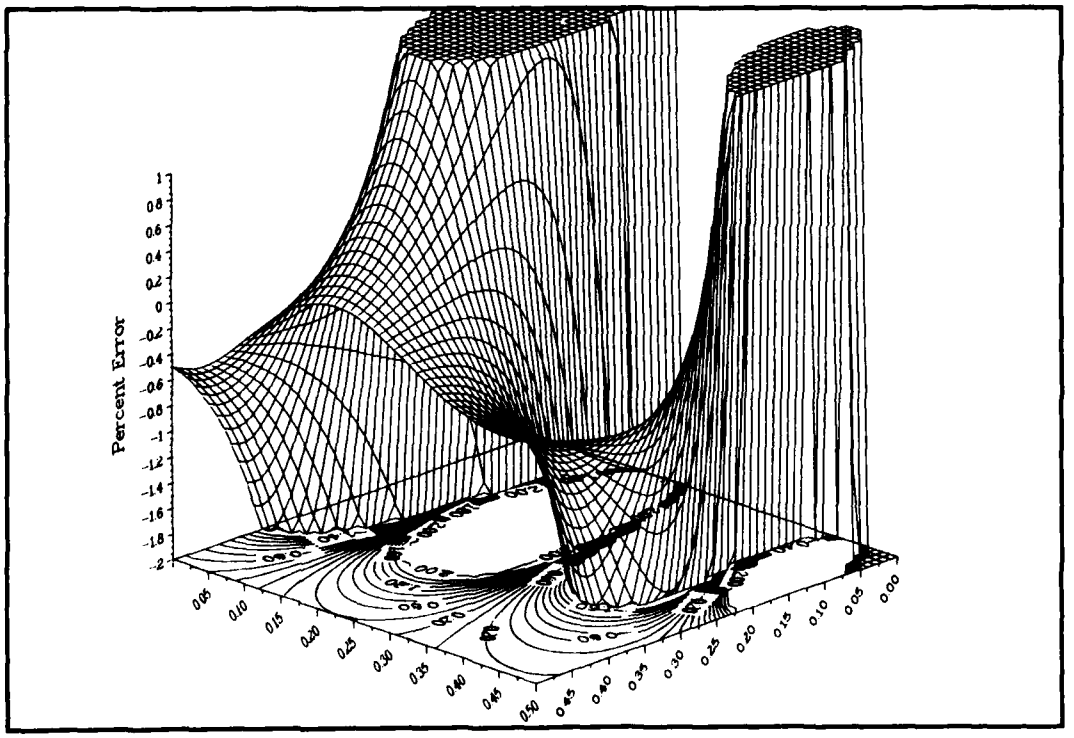

(b) σ_{11} error field.

Figure 6. Four-point integration results for a single element in an infinite plane (defined in Figure 5).

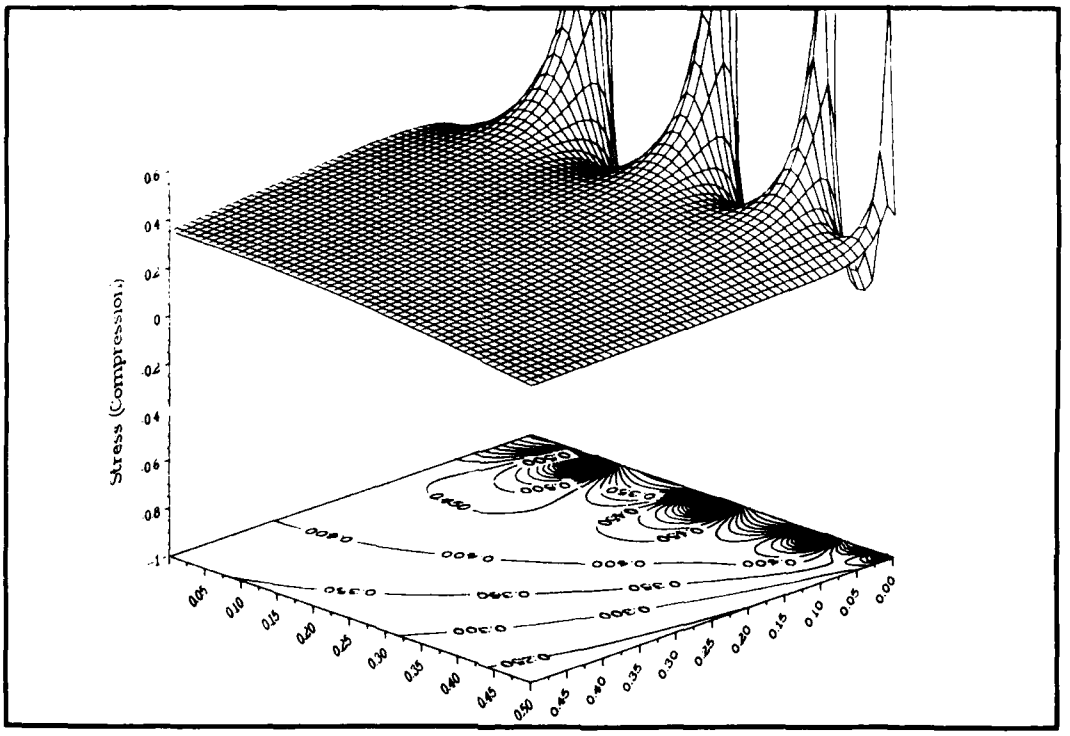

(a) σ_{11} stress field.

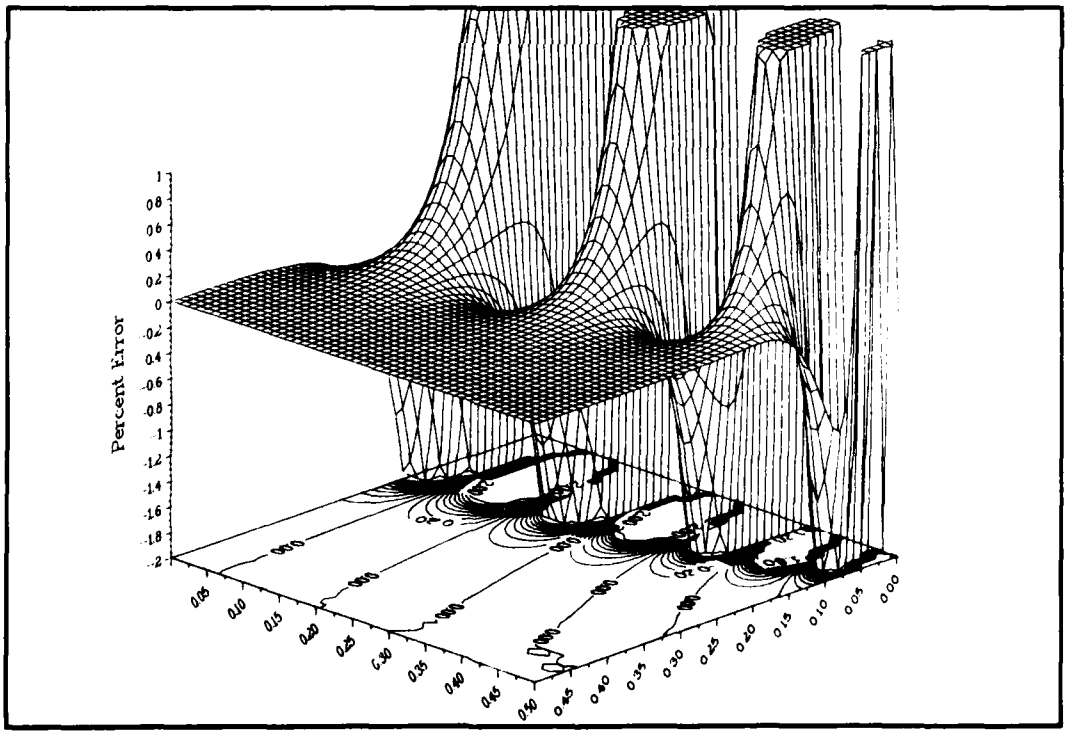

(b) σ_{11} error field.

Figure 7. Eight-point integration results for a single element in an infinite plane (defined in Figure 5).

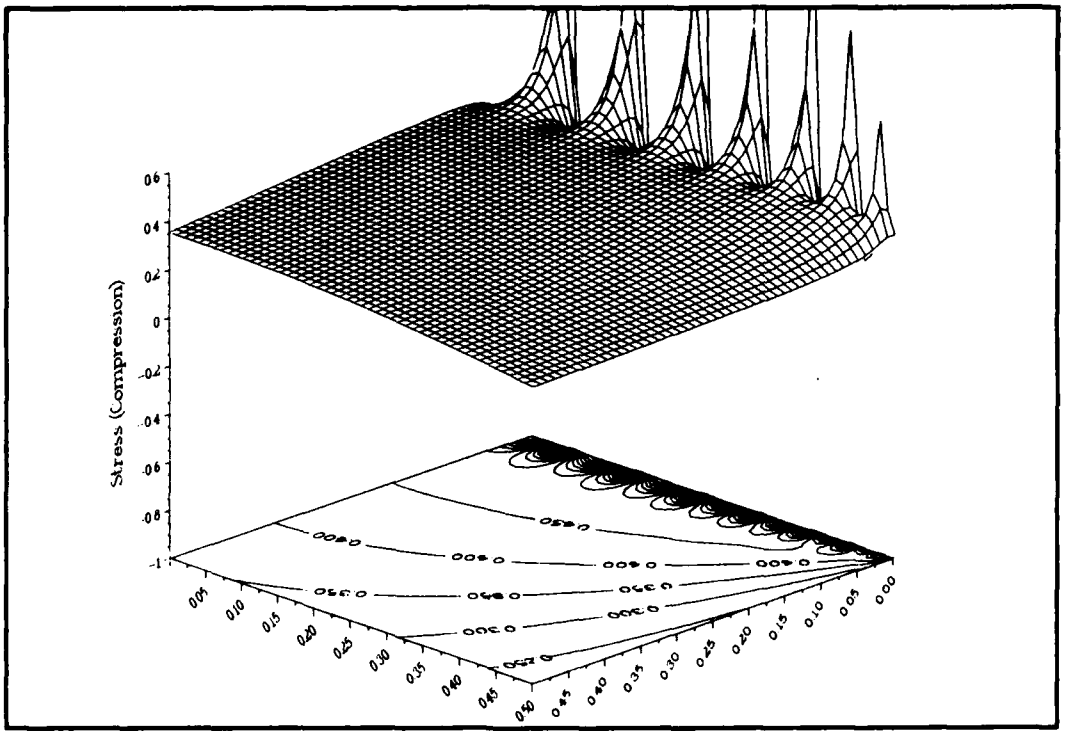

(a) σ_{11} stress field.

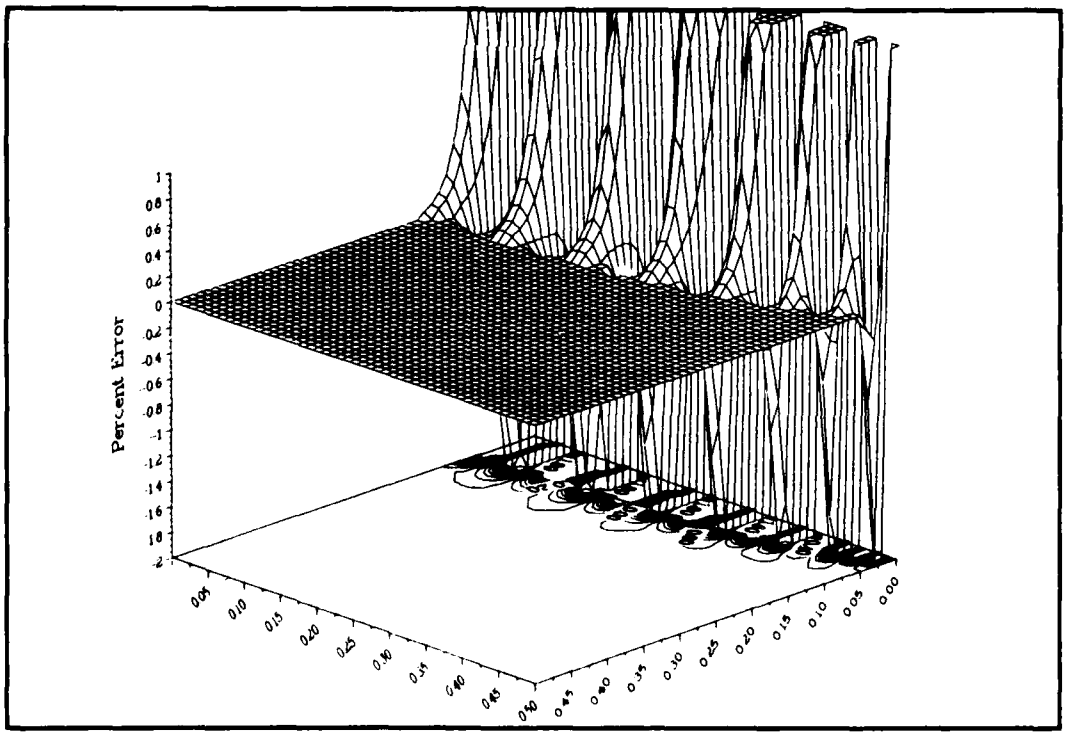

(b) σ_{11} error field.

Figure 8. Sixteen-point integration results for a single element in an infinite plane (defined in Figure 5).

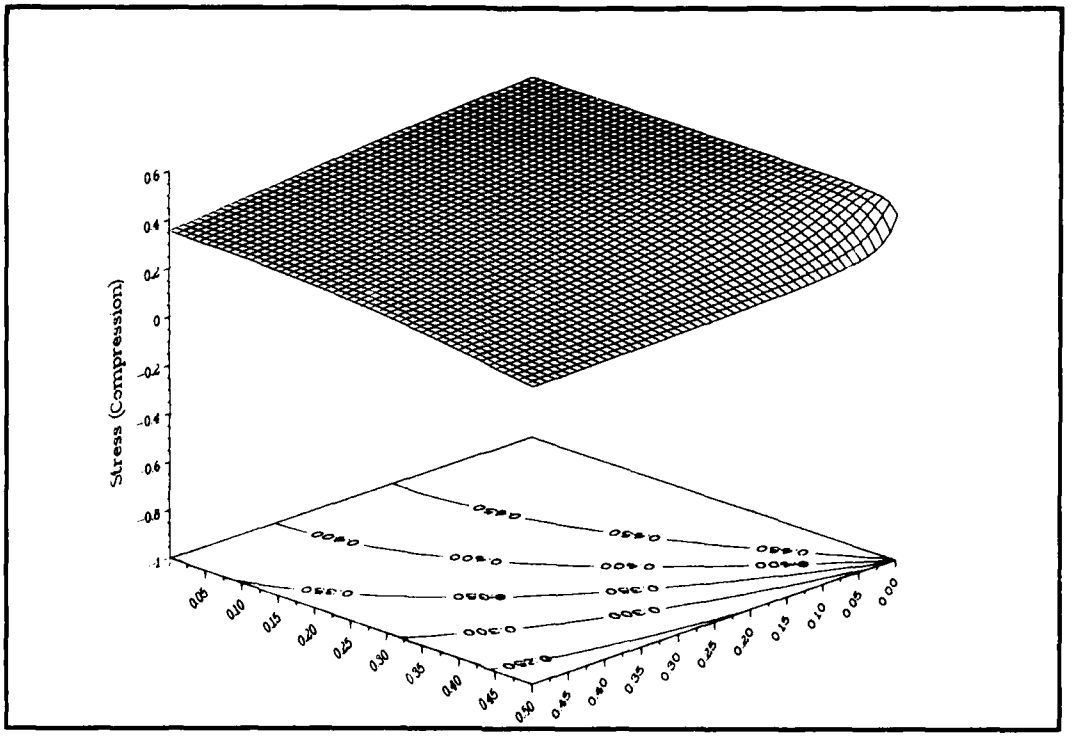

(a) σ_{11} stress field.

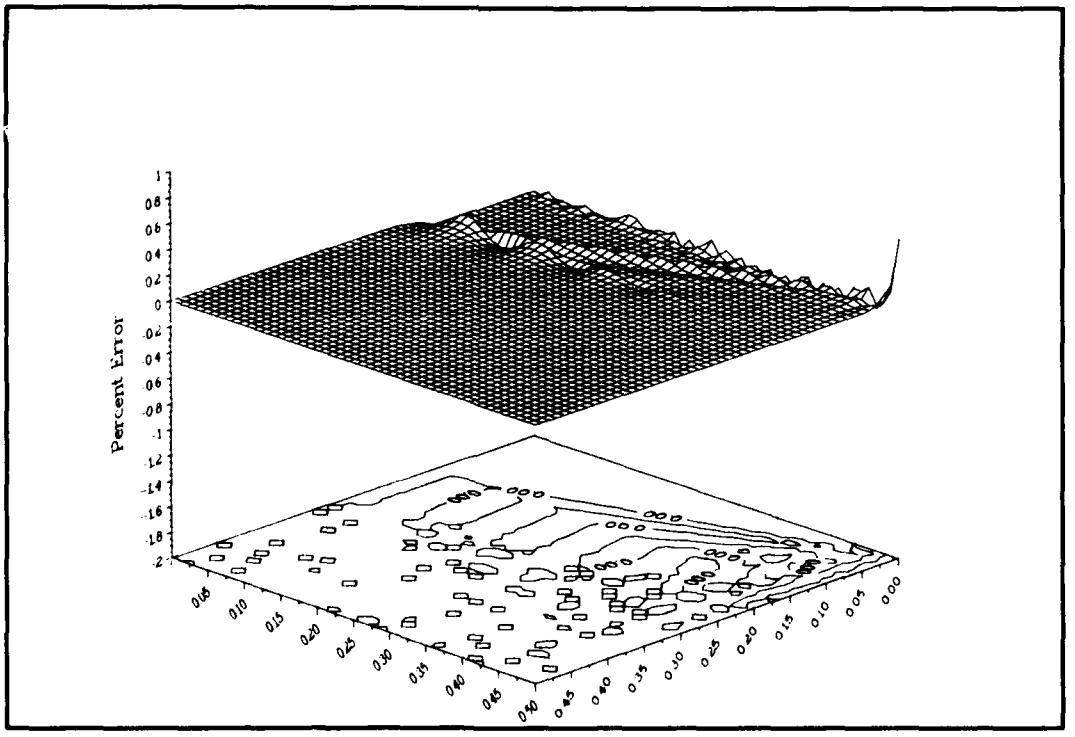

(b) σ_{11} error field.

Figure 9. Recursive integration results for a single element in an infinite plane (defined in Figure 5).

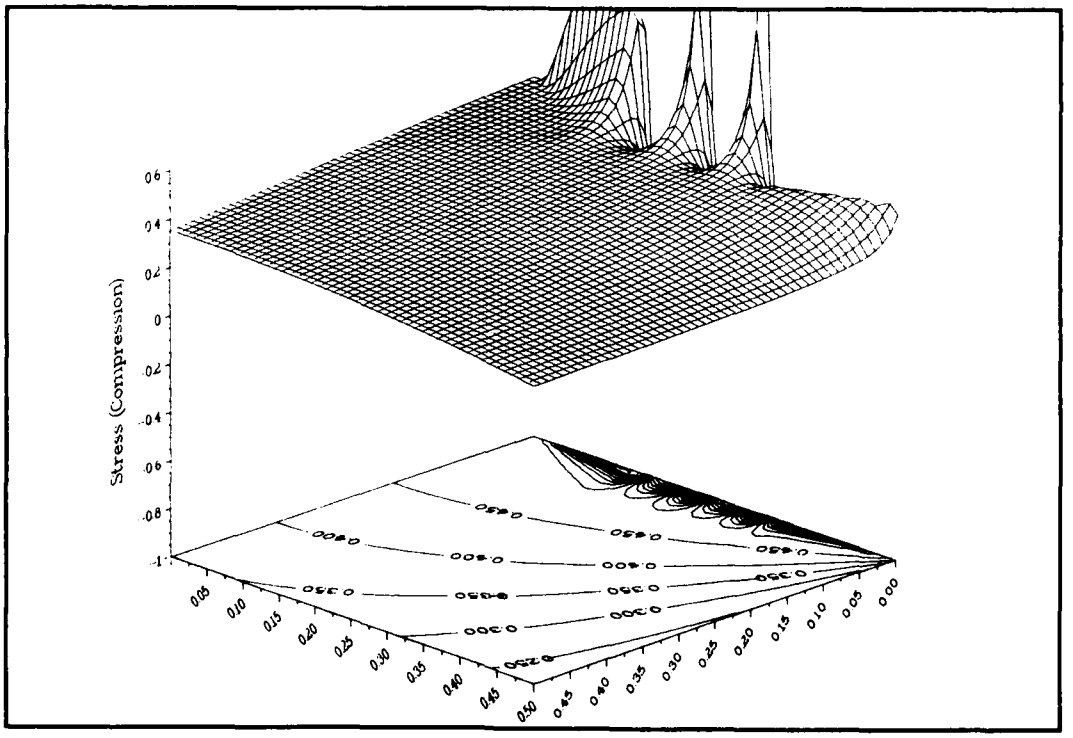

(a) σ_{11} stress field.

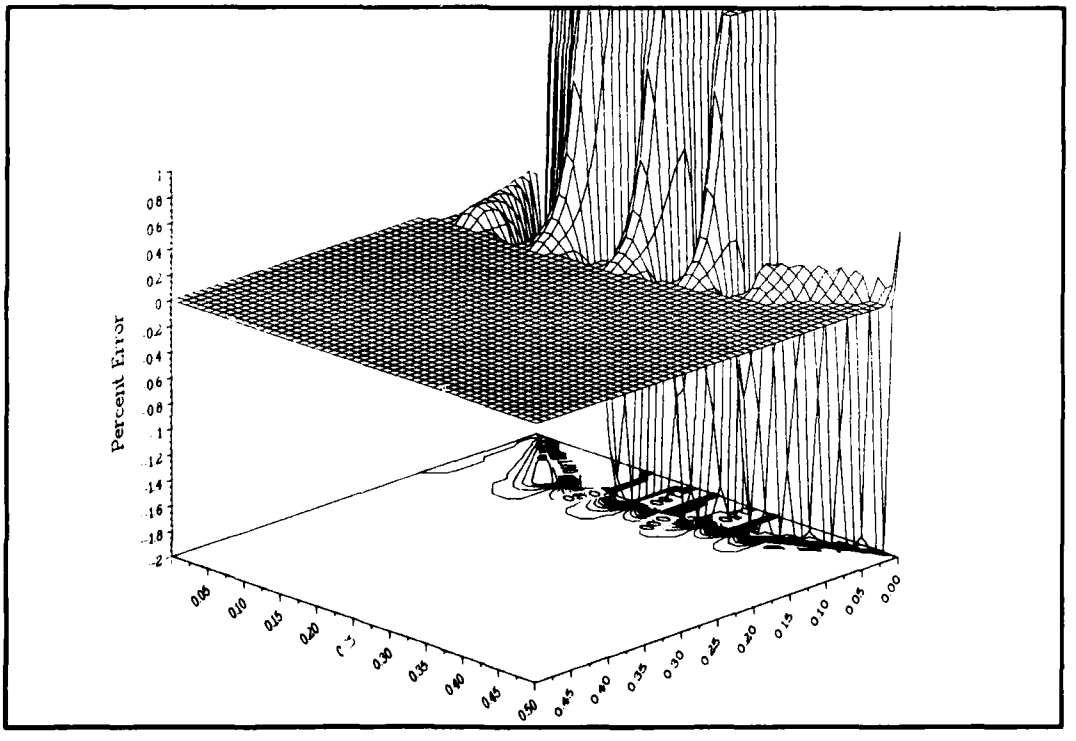

(b) σ_{11} error field.

Figure 10. Recursive integration results using the nodal radius estimate.

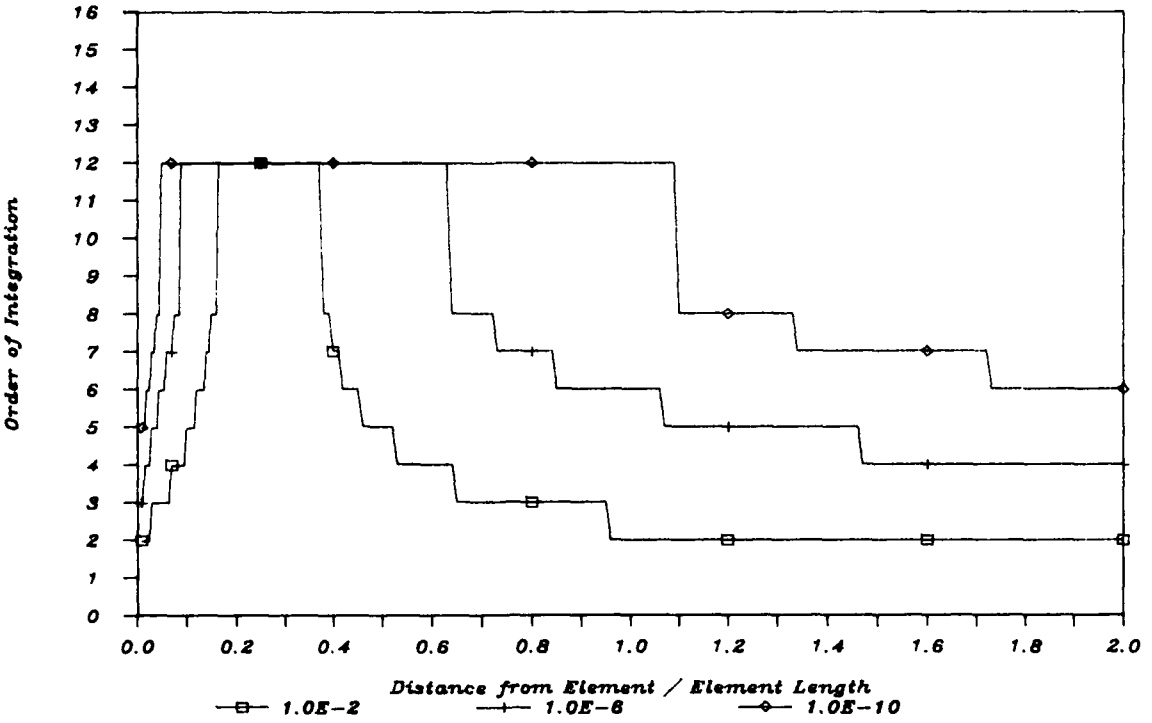

Figure 11. Banerjee and Butterfield's formula for variable-order integration.

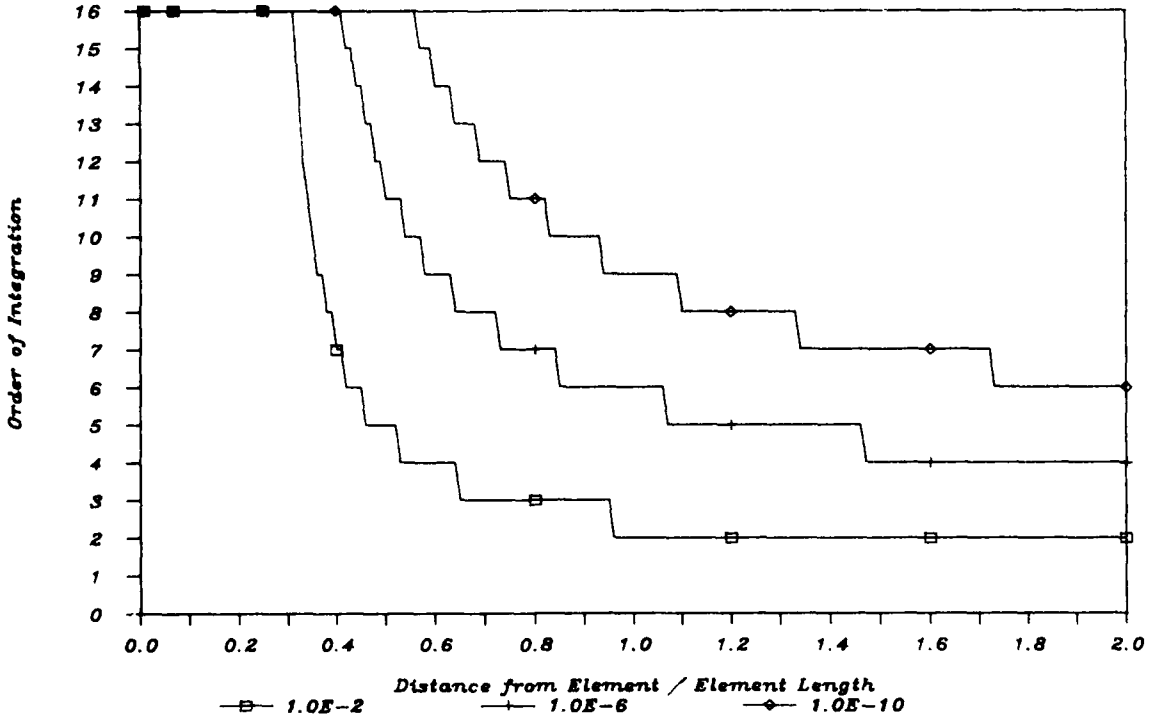

Figure 12. Revised formula for variable-order integration.

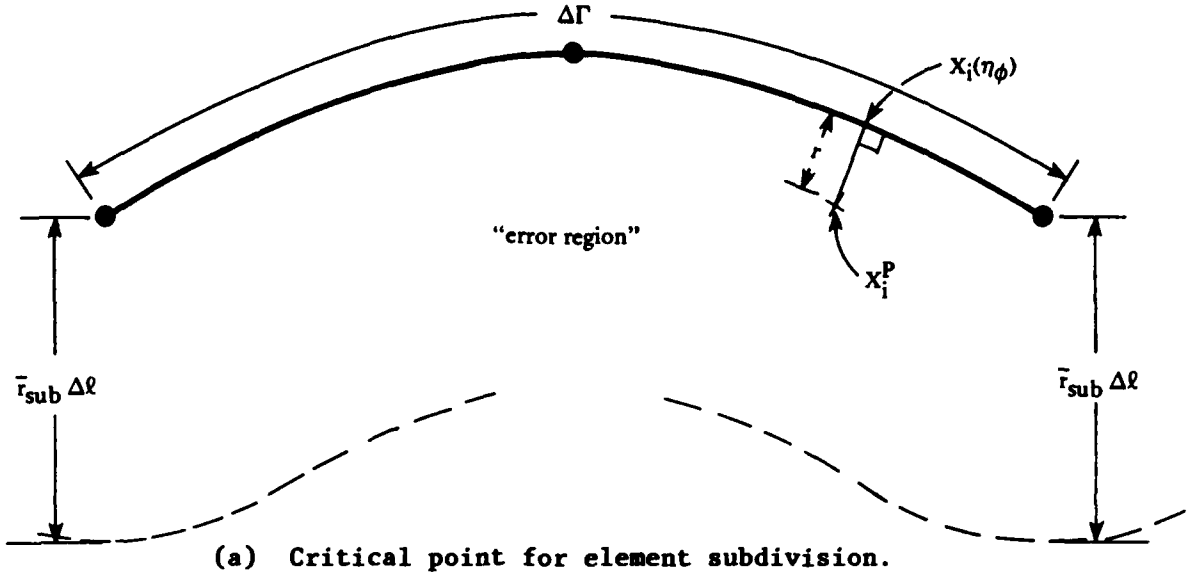

(a) Critical point for element subdivision.

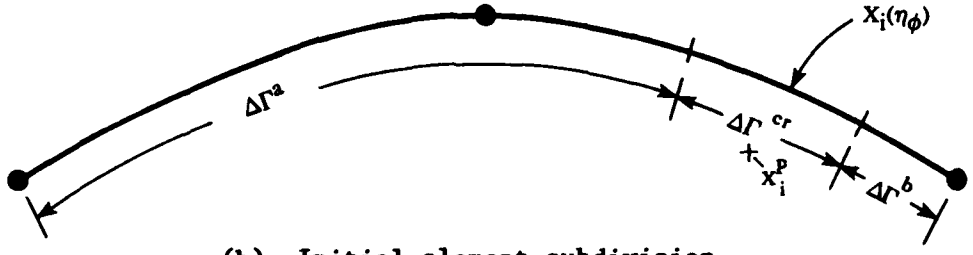

(b) Initial element subdivision.

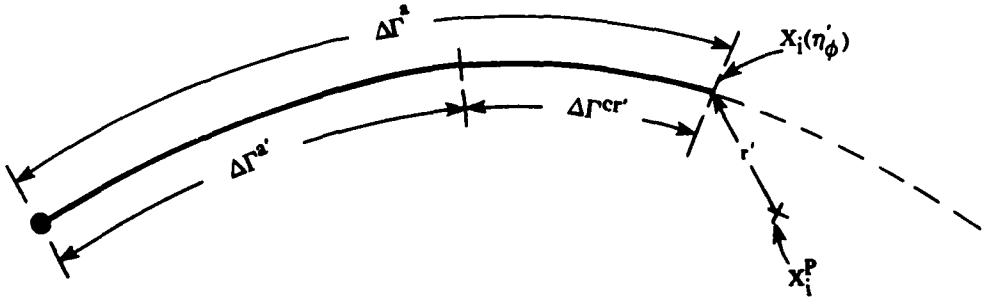

(c) Subdivision of $\Delta\Gamma^a$, the first level of recursion.

Figure 13. Recursive element subdivision.

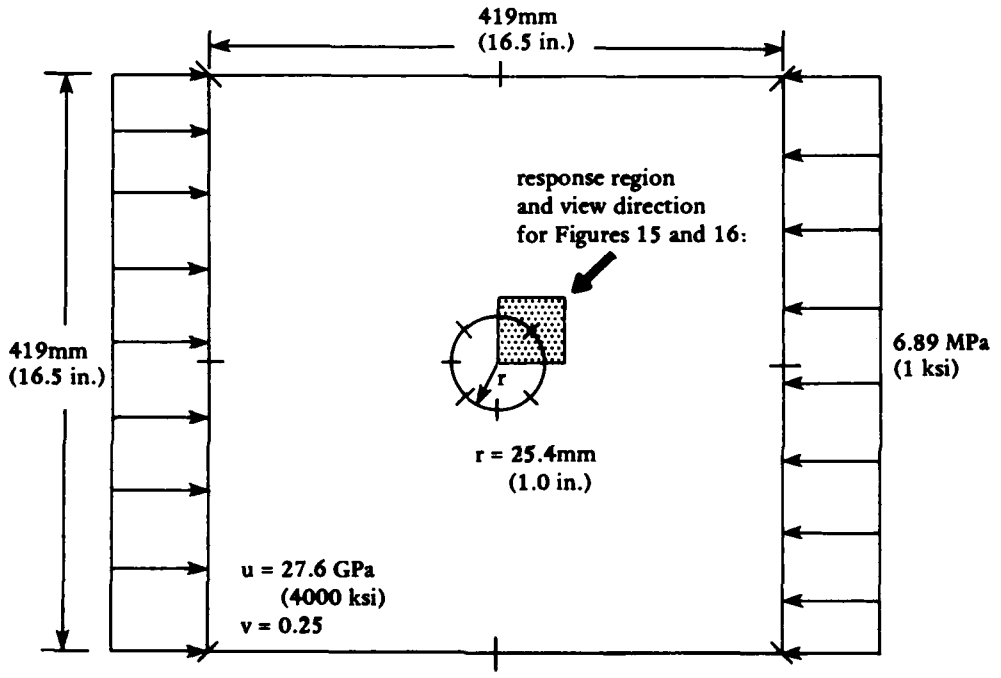

Figure 14. Hole in a plate problem.

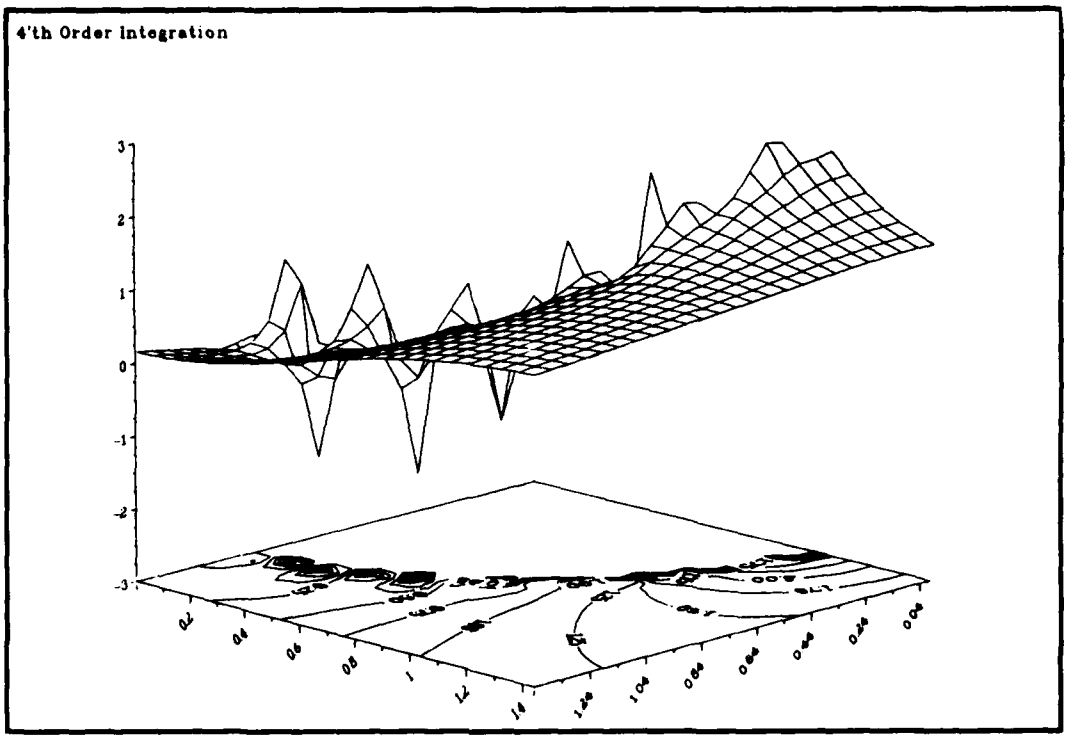

Figure 15. σ_{11} near a hole in a plate using four-point quadrature.

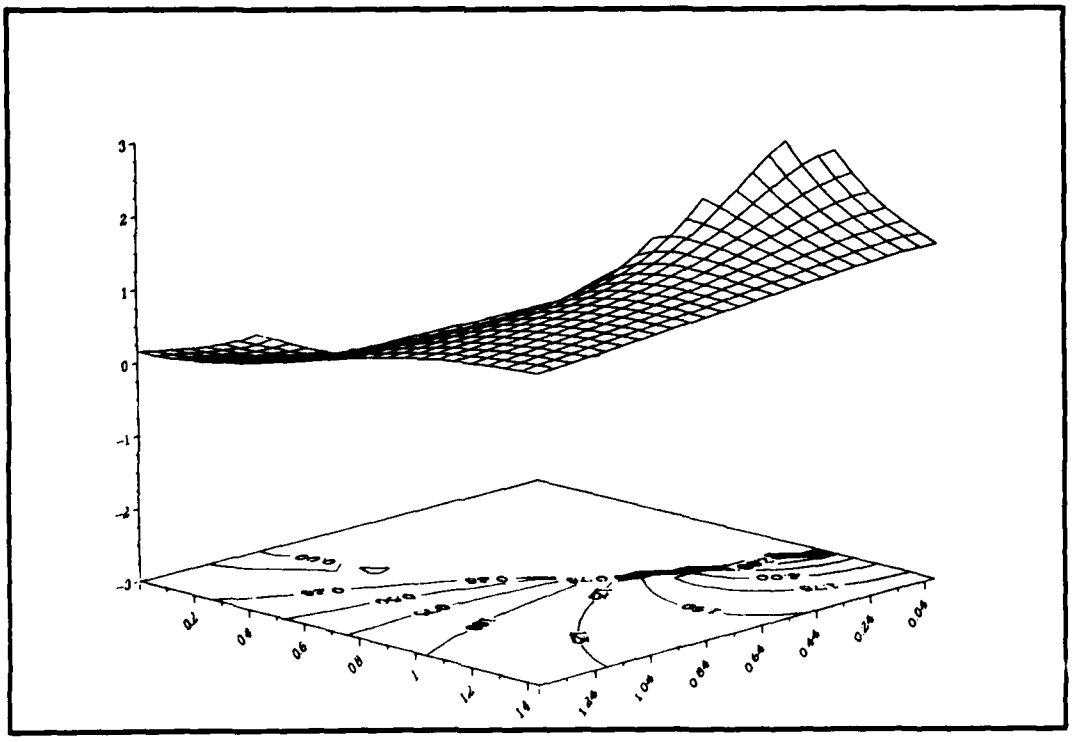

Figure 16. σ_{11} near a hole in a plate using the recursive integration technique.

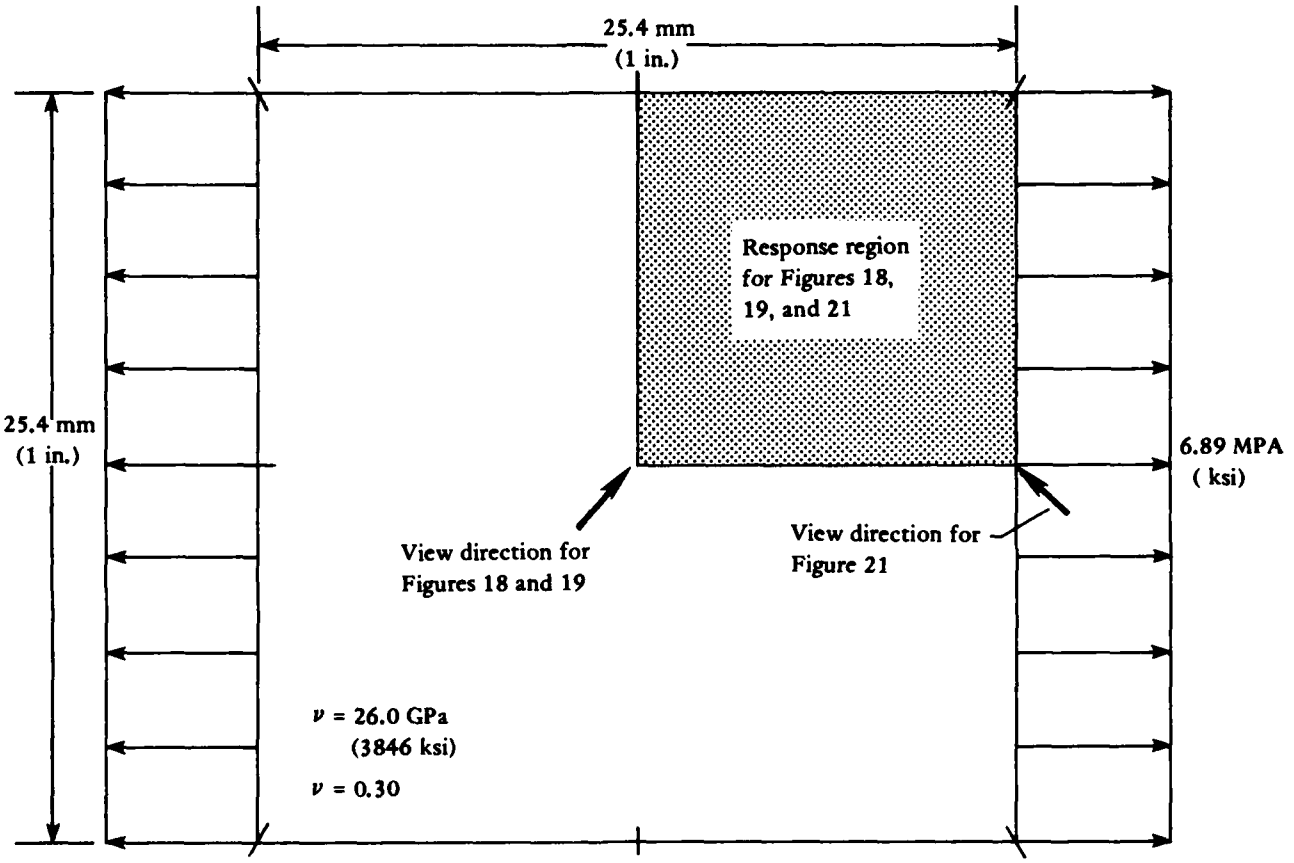

Figure 17. Square plate in uniaxial tension problem.

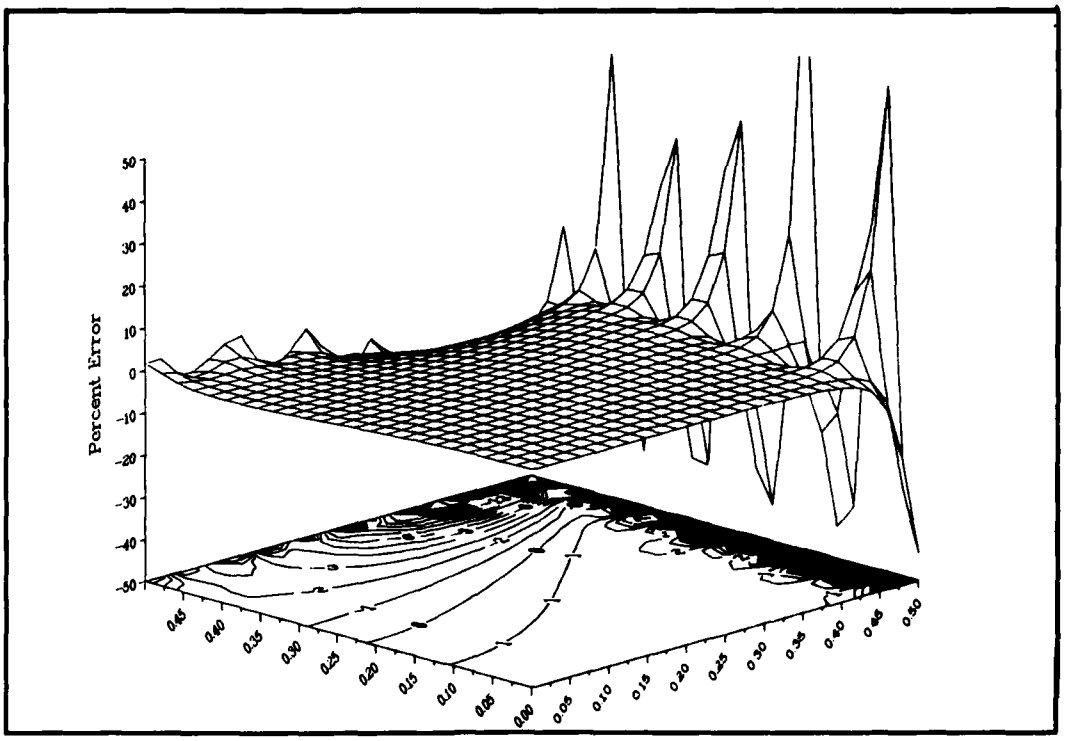

(a) σ_{11} error field without recursive integration.

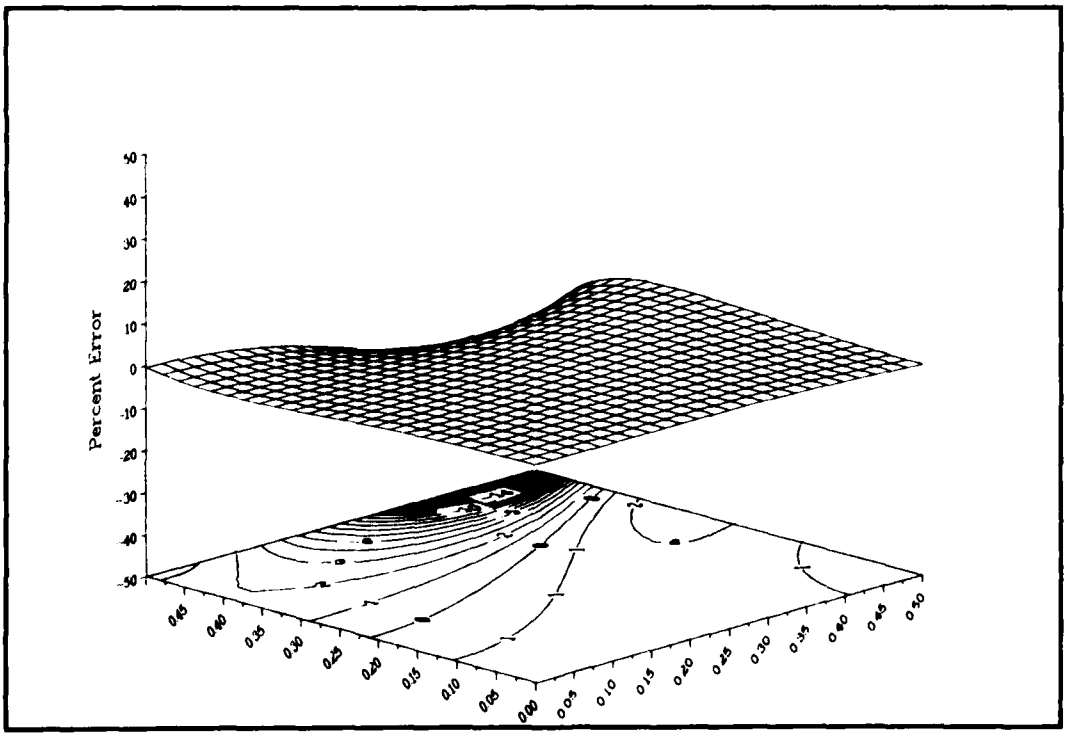

(b) σ_{11} error field with recursive integration.

Figure 18. A plate in uniaxial tension for a four-element model.

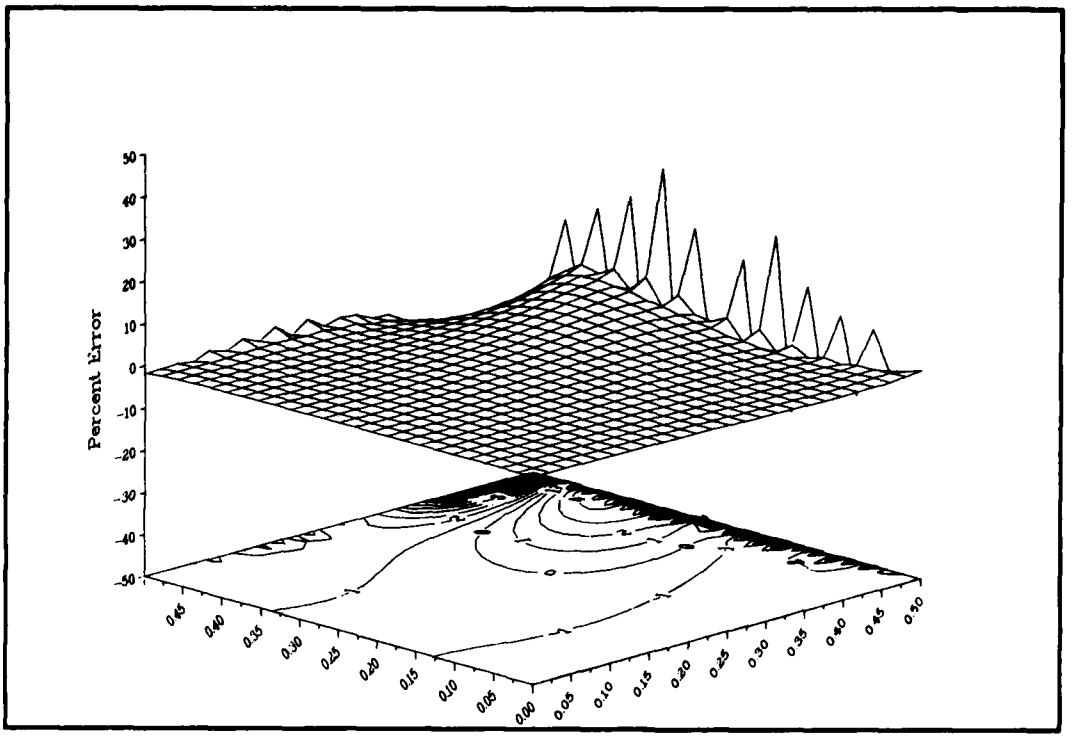

(a) σ_{11} error field without recursive integration.

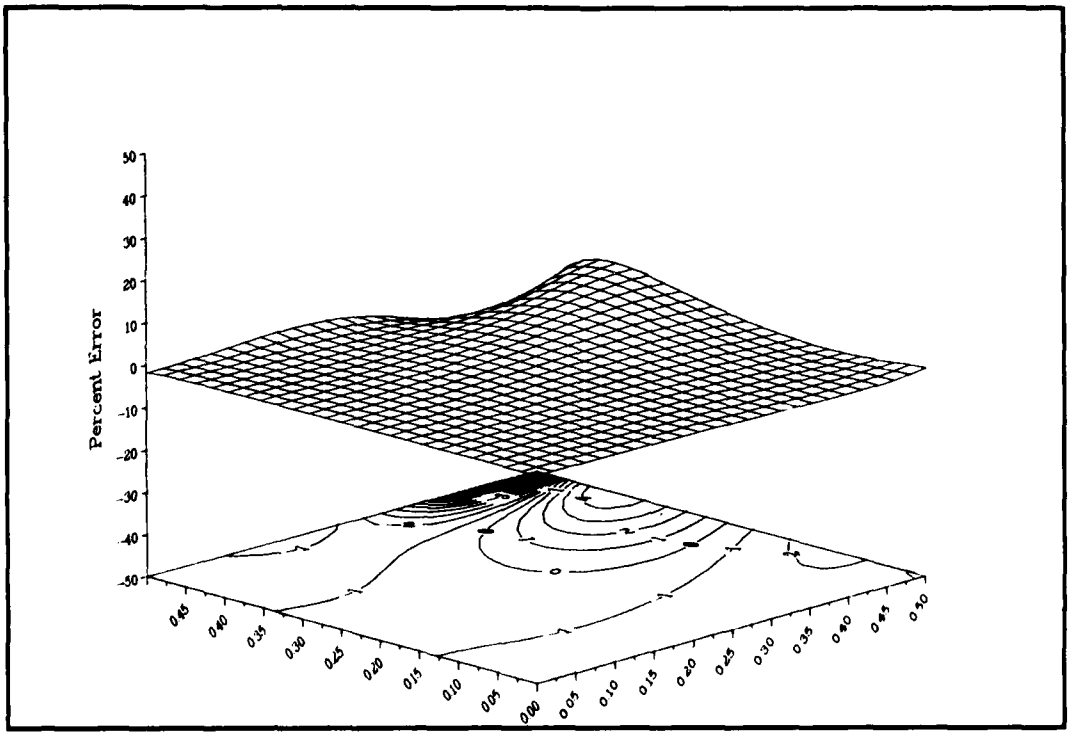

(b) σ_{11} error field with recursive integration.

Figure 19. A plate in uniaxial tension for an eight-element model.

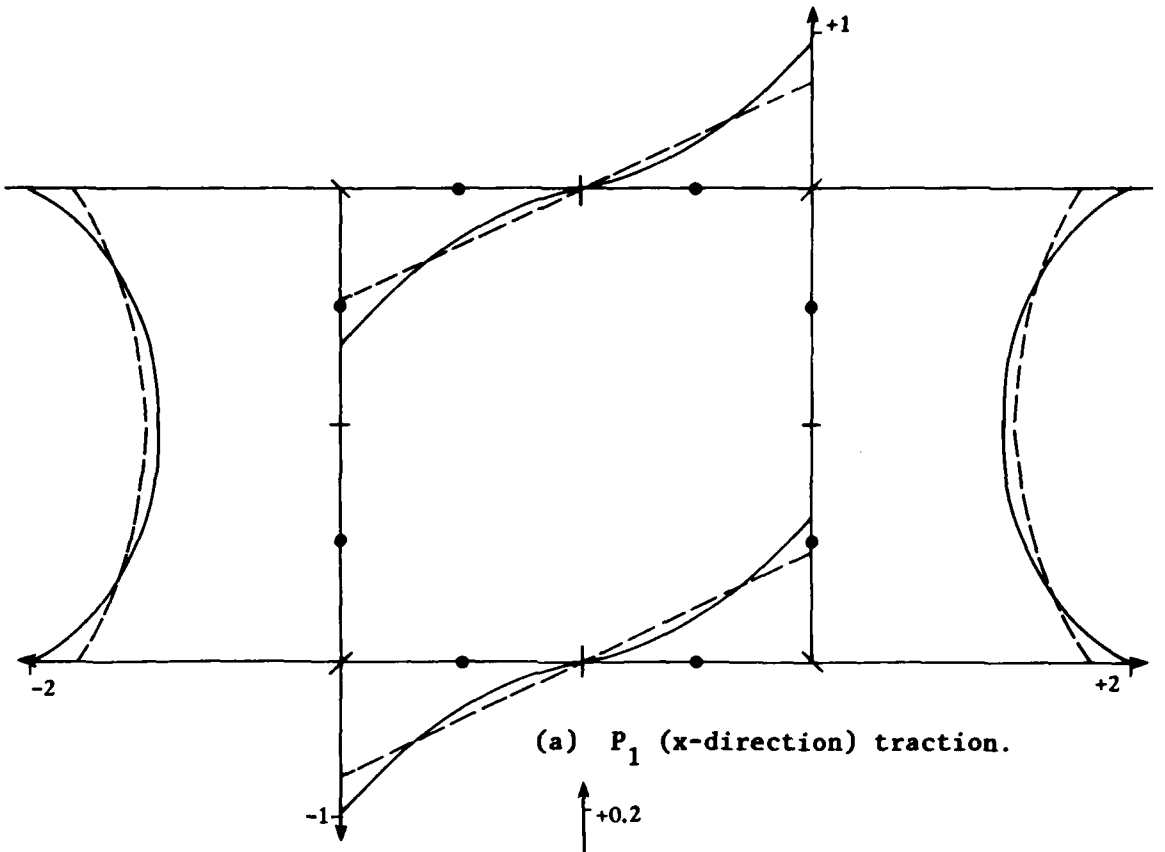

(a) P_1 (x-direction) traction.

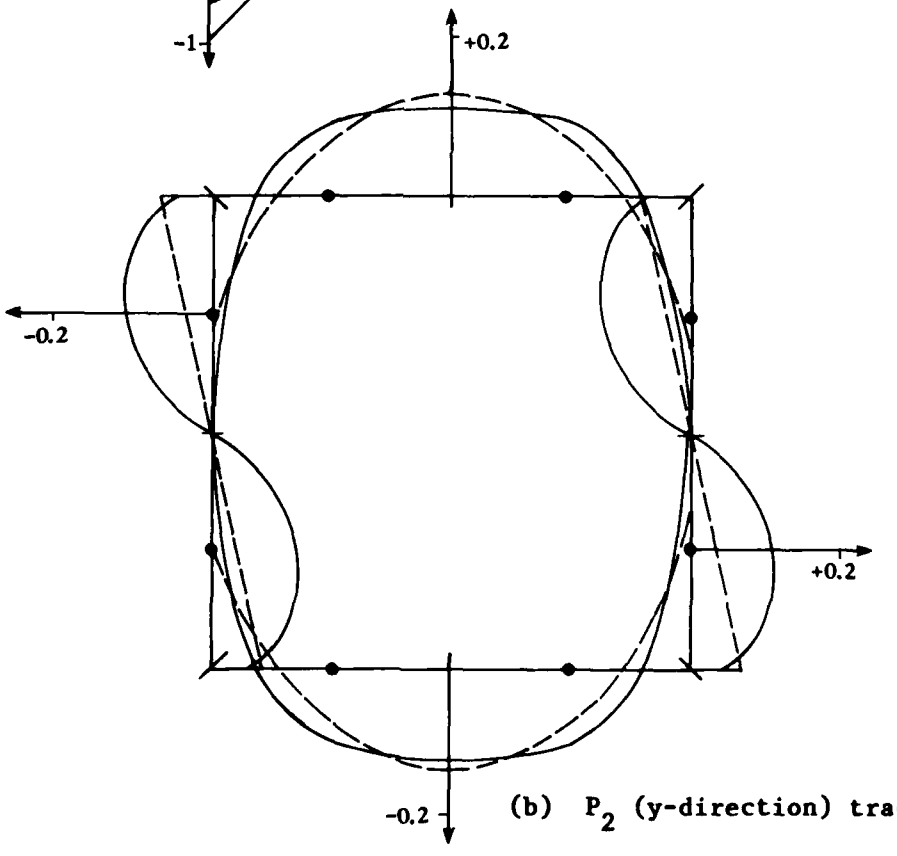

(b) P_2 (y-direction) traction.

Figure 20. Artificial boundary tractions for the plate in uniaxial tension for the four- (---) and eight- (——) element models.

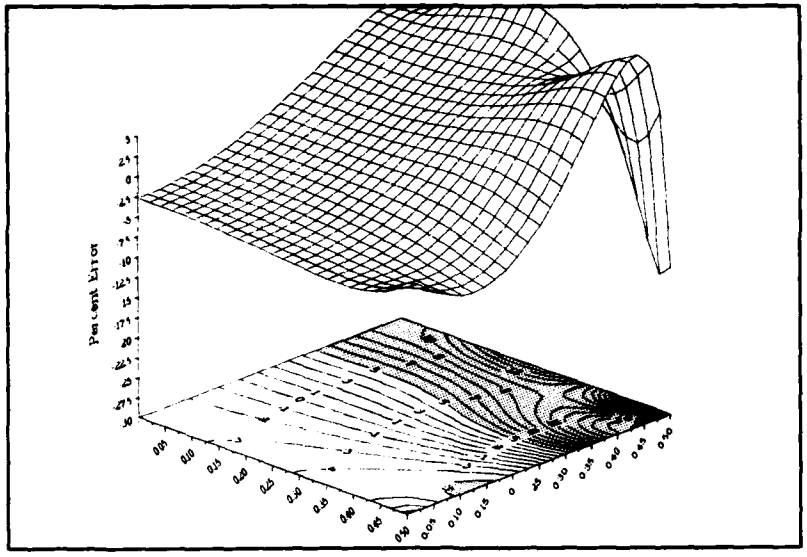

(a) $|\eta| = 0.90$.

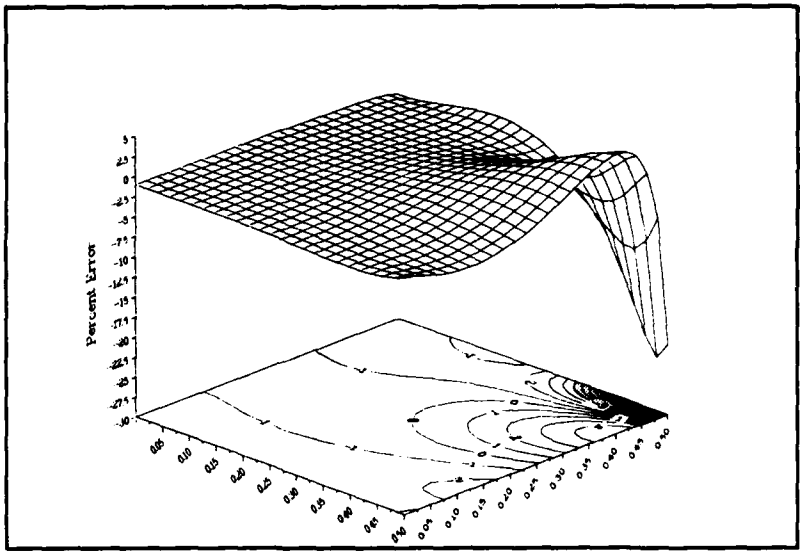

(b) $|\eta| = 0.80$.

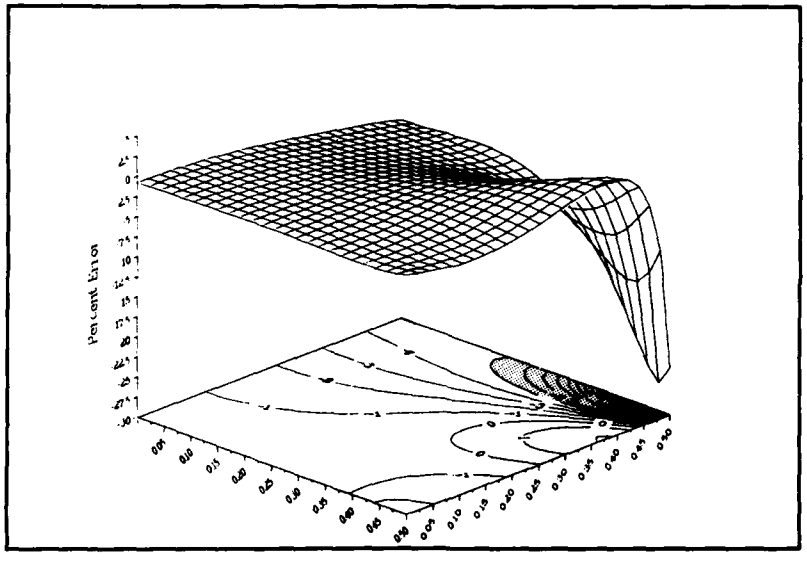

(c) $|\eta| = 0.70$.

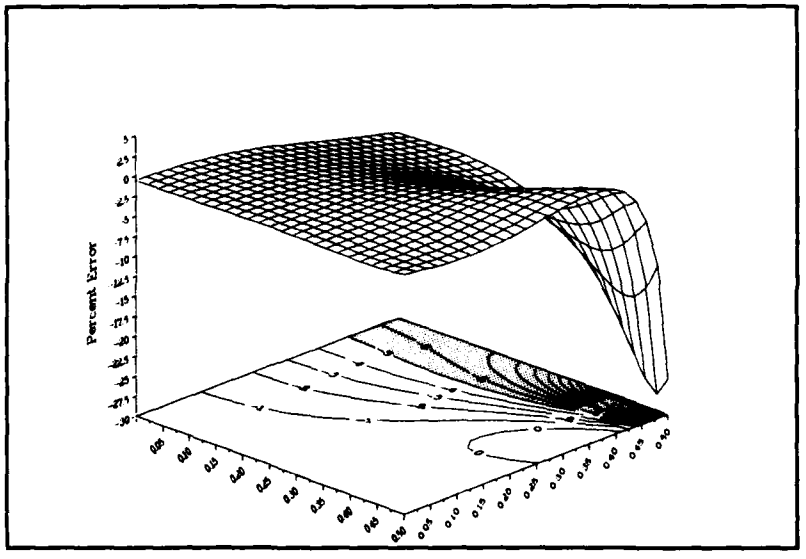

(d) $|\eta| = 0.60$.

Figure 21. σ_{11} error field for various positions of the corner collocation points.

INSTRUCTIONS

The Naval Civil Engineering Laboratory has revised its primary distribution lists. The bottom of the mailing label has several numbers listed. These numbers correspond to numbers assigned to the list of Subject Categories. Numbers on the label corresponding to those on the list indicate the subject category and type of documents you are presently receiving. If you are satisfied, throw this card away (or file it for later reference).

If you want to change what you are presently receiving:

- Delete – mark off number on bottom of label.
- Add – circle number on list.
- Remove my name from all your lists – check box on list.
- Change my address – line out incorrect line and write in correction (ATTACH MAILING LABEL).
- Number of copies should be entered after the title of the subject categories you select.

Fold on line below and drop in the mail.

Note: Numbers on label but not listed on questionnaire are for NCEL use only, please ignore them.

Fold on line and staple.

DEPARTMENT OF THE NAVY

NAVAL CIVIL ENGINEERING LABORATORY
PORT HUENEME, CALIFORNIA 93043

OFFICIAL BUSINESS
PENALTY FOR PRIVATE USE, $300
1 IND-NCEL-2700/4 (REV. 12-73)
0930-LL-L70-0044

POSTAGE AND FEES PAID
DEPARTMENT OF THE NAVY
DOD-316

Commanding Officer
Code L14
Naval Civil Engineering Laboratory
Port Hueneme, California 93043

DISTRIBUTION QUESTIONNAIRE

The Naval Civil Engineering Laboratory is revising its primary distribution lists.

SUBJECT CATEGORIES

1 **SHORE FACILITIES**
2 Construction methods and materials (including corrosion control, coatings)
3 Waterfront structures (maintenance/deterioration control)
4 Utilities (including power conditioning)
5 Explosives safety
6 Construction equipment and machinery
7 Fire prevention and control
8 Antenna technology
9 Structural analysis and design (including numerical and computer techniques)
10 Protective construction (including hardened shelters, shock and vibration studies)
11 Soil/rock mechanics
13 REQ
14 Airfields and pavements
15 **ADVANCED BASE AND AMPHIBIOUS FACILITIES**
16 Base facilities (including shelters, power generation, water supplies)
17 Expedient roads/airfields/bridges
18 Amphibious operations (including breakwaters, wave forces)
19 Over-the-Beach operations (including containerization, materiel transfer, lighterage and cranes)
20 POL storage, transfer and distribution
24 **POLAR ENGINEERING**
24 Same as Advanced Base and Amphibious Facilities, except limited to cold-region environments

28 **ENERGY/POWER GENERATION**
29 Thermal conservation (thermal engineering of buildings, HVAC systems, energy loss measurement, power generation)
30 Controls and electrical conservation (electrical systems, energy monitoring and control systems)
31 Fuel flexibility (liquid fuels, coal utilization, energy from solid waste)
32 Alternate energy source (geothermal power, photovoltaic power systems, solar systems, wind systems, energy storage systems)
33 Site data and systems integration (energy resource data, energy consumption data, integrating energy systems)
34 **ENVIRONMENTAL PROTECTION**
35 Solid waste management
36 Hazardous/toxic materials management
37 Wastewater management and sanitary engineering
38 Oil pollution removal and recovery
39 Air pollution
40 Noise abatement
44 **OCEAN ENGINEERING**
45 Seafloor soils and foundations
46 Seafloor construction systems and operations (including diver and manipulator tools)
47 Undersea structures and materials
48 Anchors and moorings
49 Undersea power systems, electromechanical cables, and connectors
50 Pressure vessel facilities
51 Physical environment (including site surveying)
52 Ocean-based concrete structures
53 Hyperbaric chambers
54 Undersea cable dynamics

TYPES OF DOCUMENTS

85 Techdata Sheets
86 Technical Reports and Technical Notes
82 NCEL Guide & Updates
83 Table of Contents & Index to TDS
91 Physical Security
☐ None—remove my name

END

FILMED

3 -86

DTIC